First of all, we would like to thank both referees (Salvatore Manfreda and one anonymous referee) that they invested their time and reviewed our manuscript in great detail to provide very constructive comments. We gladly considered each note to improve our submission.

Salvatore Manfreda (Referee)
salvatore.manfreda@unibas.it
Received and published: 19 July 2019
The main contribution of the present manuscript is oriented in exploring surface flow velocities and discharge estimations using fixed cameras and UASs devices. A full and automatic workflow is introduced for the estimation of the variables mentioned above. Two case studies are considered for validation purposes, namely the Wesenitz (paved) and Freiberger Mulde (natural). ADCP data were collected for benchmarking purposes. The manuscript is almost well written and easily understandable. Its length is also appropriate.

Major comments:

Section 2.2.1 Reference data: The authors stated that surface flow velocities were extrapolated using ADCP measurements. However, they do not say anything about the process. Please, add information on the extrapolating process. Additionally, at Wesenitz case study, only one cross-section was measured. Why such a decision? (consider that for a rigours comparison between image-velocimetry results and reference velocities is better not to use only local reference velocities).

- Thank you for your comment. We clarifed in the revised manuscript how the ADCP measurements were extrapolated. Extrapolation of surface flow velocities was performed by a procedure suggested by Adler (1993) and also described in Morgenschweis (2010). The procedure is implemented in the AGILA software; thus we believe that further details were not required. In general, it approximates a power function to the measured vertical velocity profile for each ADCP ensemble individually. Then, surface velocity (vs) is calculated by:

  $$vsi = ai * hi^{(1/6)}$$

  with h – water depth and
  a – factor (determined from measured depth-depended velocities) for each ADCP ensemble, with
  i – number of the ensemble, representing the position within the cross section.

  This means, that surface velocities were extrapolated using all velocity measurements of the ADCP. At the Wesenitz site, ADCP cell sizes of 3 centimetres were used, which resulted in up to 10 depth-depended velocity measurements per ensemble.

  - Adler, M.: Messungen von Durchflüssen und Strömungsprofilen mit einem Ultraschall-Doppler-Gerät (ADCP). Wasserwirtschaft (83) 1993, H. 4, S. 192–196.
  - Morgenschweis, G.: Hydrometrie, Springer-Verlag Berlin Heidelberg, S. 582, 2010. DOI: 10.1007/978-3-642-05390-0_1

- The Wesenitz study site is located at the gauging station. It is a straight channel with paved, trapezoidal cross sections and nearly uniform flow conditions. Thus, surface velocities vary only slightly and one cross section seems to be representative. We performed more measurements with different water depths and locations showing similar results. But we did not want to put so much focus on this because the idea of the manuscript is to compare measurements with different sensors and platforms under uniform and non-uniform flow conditions.

Section 2.2.2 Image-based data: The authors used a low-resolution camera for video acquisitions at the Freiburger Mulde case study. Justify such a decision considering that low-cost smartphones can reach a better resolution.

- Indeed, the authors used a low-resolution camera. The specific camera was originally chosen because it is also able to record high speed videos. However, analysis of these videos revealed that high speed frame rates do not necessarily improve the tracking quality but increase processing time significantly. Thus, we focused on the video with the lower frame rate, although the image resolution was low. Nevertheless, comparing our results to the ADCP measurements could still reveal the high accuracy potential highlighting that even low-resolution cameras can be used for the task of flow velocity and discharge measurements. In addition, the SLR cameras at the Wesenitz study site enabled a detailed analysis of image velocimetry with imagery with higher resolutions.

Section 2.4.3 Feature tracking: The authors stated, 'In this study, features are tracked for 20 frames and new features are detected every 15th frame'. Is there any reason for these numbers? Why did the authors decide a new detection every 15 frames?

- The decision for tracking for 20 frames and detecting features every 15 frames was chosen after evaluating different choices for tracking and detection. Although, other choices were possible (e.g. 10 frames tracking and every 10 frames detection), we settled with these settings as the results revealed steadiness and processing time was acceptable. This choice was therefore based on our experience with both rivers.
- The more frames are tracked across; the more reliable and robust tracking results are possible because the later filtering will have a larger sample for processing. However, the longer features are tracked the longer the processing time is going to be. Choosing feature detection every 15 frames allowed us to densify the final feature tracks. Features can change and new features enter the area of view although the already detected features are still tracked. Thus, it can be suitable to detect features more frequently than the number of frames they are tracked across. Thank you for highlighting the lack of explanation in the manuscript. We added this information to the revised manuscript.

Section 2.4.4 Track filtering: This subsection is relevant and deserves a better explanation of the filtering criteria. For example, it would be positive to add a figure showing an example of application of the different filtering criteria (e.g. what is the reference for the angles?).

- Thank you for your comment. In fig. 5 we already implemented four sub-figures, which show how the different filtering steps improve the tracking results. We added two more sub-figures to highlight more specifically, how the consideration of sub-track directions and the deviation from the average flow direction improves overall velocity field reliability.
- The references for the angles are chosen differently. The average flow direction is calculated from all tracks and then a buffer value is chosen to exclude tracks that exceed the average flow direction by a specified threshold. This threshold has to be defined considering the general variability of the river surface flow pattern. The other criteria concern the steadiness of the tracks. If the standard deviation of the sub-tracks is above a specific value, they are excluded because we assume a steady flow for a track. Again thresholds are chosen considering the general flow characteristic of the observed river. We added some more information to the revised manuscript regarding the choice of the thresholds.

Section 2.4.5 Velocity retrieval: The authors stated: 'The threshold is defined as the sum of the average velocity with a multiple of its standard deviation'. Please, add information about the 'multiplying factor' of the standard deviation.

- The multiplying factor has to be chosen according the quality of the filtering results. If the factor is set to a high value only a few values, which deviate strongly from the average velocity, are removed. And if a low value is chosen, many more tracks are filtered out, which might be wanted in situations, when solely the most reliable tracking results are aimed for. We added this information to the revised manuscript.

Section 2.4.5 Velocity retrieval: The authors stated: 'For a better visualisation, final flow velocity tracks are rasterized'. Please, add information about the block assumed for the rasterizing process. If the comparison of estimated velocities is made with the rasterized velocities, please mention it and discuss implications.

- In this study we assumed a block of 20 pixels. However, we did not compare the rasterized velocities. We only used the original velocity tracks for comparison to the reference to avoid inaccuracies due to interpolation errors. In this study, the rasterized data is only considered as a visualisation tool and therefore we removed it in the revised manuscript to avoid confusion. Instead, we implemented a figure that contains the final tracks and the location of the ADCP track including a buffer to identify, which features were used for velocity comparison.

Section 3.2 Flow velocity measurements at the Wesenitz: The authors stated 'However, it is difficult to perform exact comparison to the ADCP measurements because the precise location of the ADCP cross-section in the local coordinate system of the river reach is not known as the ADCP boat was not equipped with any positioning tool and its movement across the water surface was neither tracked nor synchronised. Therefore, the accuracy assessment of the spatial velocity pattern is limited'. This is a critical issue that may limit the validation of the procedure. Do you have any alternative strategy to quantify ADCP positions in order to allow a realistic comparison?

- In this study, we were able to identify the start and end points of the cross-sections in the imagery at the shore. Therefore, we could approximately estimate the locations of the cross-sections. However, the location could only be estimated in the dm-range, which allows for velocity comparison if the surface flow velocity pattern does not become too variable within shortest distances. We just wanted to highlight that this has to be kept in mind. We added this info to the revised manuscript.

Minor comments:

Page 2, Line 2: '. . .observe flash floods. And Le Coz et al. . .'. Please, remove the point before 'and'

- Thank you for the comment. We changed this in the revised version.

Page 2, Line 22: Please, consider starting a new paragraph after '. . .then searched for in the subsequent images.'.

- Thank you for the comment. We added a new paragraph in the revised version.

Page 3, Line 4: '. . .flow conditions. And Costa et al. (2000). . .'. Extra point into the sentence.

- Thank you for the comment. We removed the extra point in the revised version.

Page 4, Line 12: 'Here, average water level and discharge are 48 cm and 2.2 m 2 /s, respectively.' Mean annual variables?

- Indeed, these are annual averages. Thank you for highlighting this. We added this information in the revised version. However, please see the next comment for further details.

Page 4, Line 19: 'During this day discharge and water level were 5.7 m 3 /s and 68 cm. Considering the information provided before (Average discharge and water levels are 6.9 m 3 /s and 66 cm, respectively), why a decrease from 6.9 m3/s to 5.7 m3/s (17% of difference) is creating an increment from 66 cm to 68 cm in terms of water levels?

- We checked the numbers again. They are correct. The measured values at that day (5.7 m^3/s and 68 cm) were obtained by continuous water level measurement and application of the rating curve, which was valid during that time. However, average discharge and water levels are long-term averages based on more than 50 years of measurements. In comparison with the values of that day, we see two effects, which are responsible for the differences. First, rating curves are changing over time (At the moment, a discharge of 5.7m^3/s is assigned with a water level of 66 cm). Second, rating curves reveal a nonlinear behaviour. With increasing water level, the discharge increases stronger, which has an impact on the averages. Thus, direct comparison of both pairs of values is not possible. However, to avoid this confusion we compared the values of that day to the average values of the hydrological year 2016, which are 5,6 m^3/s discharge and 65 cm water level, which also changed for the Wesenitz case study to obtain consistency.

Page 5, Line 19: '. . .the performance of different cameras (fig. 1b). Two. . .'. Fig. 1a?

- Indeed, this would be figure 1a. Thank you for noticing. It was changed in the revised manuscript.

Page 6, Line 31: '. . .to matching failure. And if moving. . .'. Extra point into the sentence.

- Thank you for your comment. We corrected this in the revised version.

Page 9, Line 10: '. . .suitable at the Wesenitz. But at the Freiberger. . .'. Extra point into the sentence.

- Thank you for your comment. We corrected this in the revised version.

Table 2: What is s0?

- s0 is sigma 0 and it is a resulting quality parameter of the adjustment of the spatial resection. It provides information about how well observed values fit to the adjusted values. We added this information to the table heading.

Page 11, Line 29: '. . .2.7 m 3 /s, which corresponds to the velocity measured by the ADCP. . .'. Discharge.

- Thank you for noticing. We changed this to discharge in the revised version.

Anonymous Referee #2

Received and published: 24 July 2019

This article presents a procedure to extract surface flow velocities and flow discharge from images captured either with permanent cameras or with drones in natural water systems. The methodology includes i) vibration removal from captured images, ii) feature identification with the GFTT algorithm, iii) feature tracking and trajectory development with normalized cross-correlation, iv) trajectory filtering based on a set of predetermined rules, and v) velocity estimation. Flow discharge can be estimated by reconstructing the bathymetry with structure-from-motion techniques and utilizing a velocity coefficient to estimate depth-averaged velocity.

The manuscript does not represent a substantial contribution to scientific progress by introducing new concepts, ideas, methods or data. Most of the algorithms applied in the procedure are well known and share similarities with existing literature (see, For instance, Perks et al., 2016, Cao et al., 2018 and Tauro et al., 2018). Flow discharge measurements have already been demonstrated from Unmanned Aerial Vehicles (UAVs), see, for instance, Detert et al., 2017. Finally, several tools exist for flow calculation (see, for instance, Fudaa-LSPIV and RIVeR by Patalano et al.).

However, I acknowledge that a limitation to the implementation of image-based measurements is the lack of user-friendly and widely shared toolboxes. In this vein, the manuscript addresses the relevant scientific issue of establishing a procedure that can guide the users from image acquisition to flow discharge calculation. In this respect, the manuscript may be appreciable to the HESS readership as a technical note, and provided the focus of the article is targeted on the presentation of the tool and on its performance. Regarding the scientific quality and validity of the applied methods, many details are missing and, in its current form, it is difficult to evaluate the scientific soundness of the work. Additional experimental and analytical justification and, sometimes, data would be mandatory to establish a novel procedure. Finally, the presentation of the work should be improved as well as several figures.

- Thank you very much for you detailed notion on our manuscript. Indeed, we did not aim at presenting a completely new concept regarding image velocimetry, as we also referred to the literature in the manuscript. We rather focus on improving existing methods, e.g. such as so far missing automatic image co-registration approaches (including performance assessment) or automatic extraction of feature search areas considering the water surface and river topography to improve the robustness and processing time of feature tracking. We believe that these improvements are relevant scientific contributions as they are important for an increased flexible application also for non-experts in image velocimetry. However, in the revised manuscript we listed the already existing tools for completeness. Furthermore, although various literature regarding image velocimetry already exists, we believe, there is still a contribution missing that demonstrates the applicability of PTV from terrestrial as well as UAV perspectives revealing the flexibility of the method.
- We focus our study on introducing the velocimetry tool. Therefore, we chose two different study sites with uniform and non-uniform flow conditions to evaluate the chances and limits of our tool. Furthermore, although some usable tools already exist for image velocimetry, they are not all capable to perform the whole processing chain (image stabilization, automatic feature search area extraction, feature detection, tracking with PTV, filtering and scaling tracks) in one tool considering GCPs or direct camera position/orientation information for referencing. Due to the focus on the tool and data processing, we submitted our manuscript as a technical note, which the reviewer also acknowledges would be suitable and useful to the HESS reader.
- We present the tool and evaluate its performance with independent ADCP measurements at two sites. However, within the revised manuscript, we focused even stronger on the tool itself and how it can be used. And we explained further what the limits/constraints of our tool are, what pre-requisites/input are needed, and what results can be expected.
- Regarding the statement that details are missing to validate the quality and validity of our method, we are afraid that we would need a more detailed explanation what is missing. We do not believe that additional experiments or data is necessary as we already demonstrate with two different sites, revealing different flow and topographic characteristics, the suitability of our tool and discuss where the limits are (e.g. irregular profiles where no hydraulic modelling is considered to improve the estimation of the velocity coefficient). Furthermore, we do not aim to develop a completely new approach but rather improve and combine existing

velocimetry tools, which is stated in the last paragraph of the introduction as well as in the added section 'Limits and perspectives'.

- In the revised form we are more specific regarding the tool, improved the readability, and we improved figures, where needed.

In the following, I report major comments.

1. An important flaw of the work is that the computational tool is barely presented and recalled to during the manuscript. Since the focus of the paper is the introduction of a new procedure, the work should clearly state the underlying assumptions of the algorithms, required data and expected outputs. Some of these points are only mentioned briefly in the supplementary material and they are not given the right visibility. For instance, I believe it should be made clear that the water level is an input to the procedure, as well as a decent number of ground control points. The sentence "the provided velocity tracking tool allows for a contact-less measurement of spatially distributed velocity fields and to estimate river discharge in previously ungauged and unmeasured regions" should, therefore, be properly edited. Another important point regards the limitations of the procedure with respect to required inputs. For instance, it looks like images need to capture river banks in order for image co-registration to be effective. This is a remarkable limitation and it should be clearly stated for users and readers.

- Thank you for this comment. In the revised manuscript we referred more closely to our tool. Furthermore, different processing stages (e.g. expected output, required data) are also explained in the tutorial of the tool, which is in the supplemental material of the manuscript.
- If the camera position/orientation is known (e.g. from precise GNSS and IMU information), actually no GCPs are needed. This missing information is provided in the revised manuscript.
- We adjusted the sentence concerning the application in ungauged regions in the regard that of course some scaling information is needed.
- We already state and discuss in the manuscript that the shore line of the river has to be visible (p 7 l 2-3, p 10 l 1-3). However, we discussed some more the corresponding limit that very wide rivers could solely be observed from high flying altitudes (potentially reducing the visibility of features to track) or with cameras with wide opening angles (potentially resulting in stronger lens distortions, which however can be corrected with suitable calibration procedures).

2. Since the Authors claim that a new procedure is being introduced, a motivation on the selection of the specific sites should be provided. If the sites mostly differ in the morphology of their river bed, the bathymetry of both of them should have been independently (that is, not with images) measured and considered as a benchmark for structure-from-motion results.

- We would like to highlight that we do not claim that a new procedure is introduced. We state for instance that we rely in PTV and Shi-Tomasi feature detection. We solely claim that our approach is automatic in most regards and that it is independent from the acquisition perspective.
- Indeed, both study sites were chosen due to their morphological differences. However, the focus of our study is not on SfM because we only consider it as a further tool. Therefore, we refer to a previous study by Dietrich (2017), who demonstrated the usability of SfM for bathymetry, instead of establishing another benchmark. In another study (Eltner et al, 2018) we were able to demonstrate the usability of SfM to measure the bathymetry (actually at the same gauge at the Wesenitz comparing SfM to a cross-section measured with total station resulting in deviation below). We added this information to the revised manuscript to further acknowledge the suitability of our approach.

    - Dietrich, J.T.: Bathymetric Structure-from-Motion: extracting shallow stream bathymetry from multi-view stereo photogrammetry. Earth Surface Processes and Landforms, 42(2), 355-364, 2017

- Eltner, Anette, Elias, M., Sardemann, H., Spieler, D.: Automatic Image-Based Water Stage Measurement for Long- Term Observations in Ungauged Catchments. Water Resources Research, (54), WR023913, 2018

3. Details on the ADCP benchmark measurements are missing. For instance, it is not clear how surface flow velocities were extrapolated from a range of 14 cm near the water surface. Given the rather shallow depth of both streams, it is surprising the Authors did not try to reconstruct the full velocity profile with the ADCP. Wind effects are not mentioned as well as alternative possible sources of noise in the data.

- Because Salvatore Manfreda made a similar comment regarding the ADCP measurements, we copied and pasted our answer to review 2:
- We clarified in the revised manuscript how the ADCP measurements were extrapolated. Extrapolation of surface flow velocities was performed by a procedure suggested by Adler (1993) and also described in Morgenschweis (2010). The procedure is implemented in the AGILA software; thus we believed that further details were not required. In general, it approximates a power function to the measured vertical velocity profile for each ADCP ensemble individually. Then, surface velocity (vs) is calculated by:

$$v_{si} = a_i * h_i^{(1/6)}$$

with h – water depth and
a – factor (determined from measured depth-depended velocities) for each ADCP ensemble, with
i – number of the ensemble, representing the position within the cross section.

This means, that surface velocities were extrapolated using all velocity measurements of the ADCP. At the Wesenitz site, ADCP cell sizes of 3 centimetres were used, which resulted in up to 10 depth-depended velocity measurements per ensemble.

- Adler, M.: Messungen von Durchflüssen und Strömungsprofilen mit einem Ultraschall-Doppler-Gerät (ADCP). Wasserwirtschaft (83) 1993, H. 4, S. 192–196.
- Morgenschweis, G.: Hydrometrie, Springer-Verlag Berlin Heidelberg, S. 582, 2010. DOI: 10.1007/978-3-642-05390-0_1

- Thank you for your advice regarding sources of noise in the data. We added this in the discussion since this is also a general limitation of all measurement systems relying on surface velocities. During our measurement campaign, we had nearly windless conditions.

4. The description of the optical experimental setup is also unclear. The orientation angles of the optical axes of the cameras are not provided. Also, in case of experiments on the Wesenitz, even if three terrestrial cameras are installed along the cross-section, none of them captures the entire width of the stream. Using diverse optical parameters for the cameras could have been interesting if results had been better discussed and referred to such settings.

- Thank you for your comment. In the revised manuscript, we provided an appendix that contains the information about the exterior orientation parameters (including the accuracy). We did not include it in the original manuscript because we did not see the relevance of further discussion of the orientation parameters. In contrast, we wanted to show that our approach is independent of the exterior orientation of the camera, as long as it can be determined (either by direct geo-referencing or indirect from control points).
- We would like to note that all three terrestrial cameras at the Wesenitz capture the entire width of the stream. However, there might be a confusion if fig. 8 is considered to assess the stream coverage. Unfortunately, the right shore is not completely displayed, although it has been captured (e.g. see fig. 3,

displayed for camera 1200D-I, and compare to fig. 8), because features were not detected at the right shore (due to missing floating particles and sun reflections) and therefore we overlaid the legend over the right shore to save some figure space. We added this notion to the revised manuscript.

5. Most of the presented algorithms share common traits with already published material. However, some of them introduce novel aspects whose accuracy is not adequately assessed in the manuscript. Was the co-registration tested elsewhere before? Was it tested in windy conditions, under different camera orientations/frequencies/resolutions? What about the feature search area and pose estimation? What are the parameters such procedure is sensitive to? Was it validated in diverse conditions? If the method was only tested in the two case studies reported in the paper, then how can this tool be regarded as a robust alternative to thoroughly tested and used ones?

- We would like to state that we think, we could show in our study the usability of the automatic co-registration approach by comparing it to chosen control points (fig. 7). Furthermore, the accuracy and suitability of co-registration in different conditions over longer periods of time has been tested and illustrated in Eltner et al. (2018). We added a reference to that study in the revised paper. We also tested the co-registration under conditions of strong changes of orientation with lower image capture frequencies (2 per second) at another site, not included in this manuscript, and co-registration was performing well. However, we would like to note that in general as long as the shore is visible and provides enough texture in the images, co-registration works as the feature detection, matching and application of a transformation has been shown in many areas of application, also outside the environmental sciences as it is a standard approach.
- The pose estimation accuracy has already been provided in table 2 in the original manuscript. The accuracy of pose estimation depends on the distribution and accuracy of GCP measurement in object and image space. We provided some more information regarding basic principles of photogrammetric measurement in the revised manuscript.
- We are afraid that we are not sure what thoroughly tested and used alternatives the reviewer refers to. We refer our approach to existing velocimetry tools. And we are not aware of extensive (published) testing of other velocimetry tools. Most studies also solely evaluate their results at selected sites (e.g. Perks et al., 2016, Tauro et al., 2018, Detert et al., 2017). Furthermore, we apply the already tested PTV and GFTT approach and do not claim to develop a new detection and tracking tool but rather improve and combine existing methods.

6. Some of the velocimetry phases require the definition of threshold values. It is not clear if they can be edited based on the specific case study. Even if this is possible, I believe the Authors should provide some guidance for the selection of appropriate values. For instance, what are nearest neighbor area dimensions that allow to find strong clusters of particles? Or which is a suitable number of particles? I believe such parameters are highly dependent on the specific experimental conditions, and automatic ways of computing them may be developed rather than asking for an intensive visual inspection of images by the users. Similarly, are search area dimensions pre-defined or inputs to the workflow? Introducing search area dimensions automatically poses constraints on the admissible frequencies and, therefore, flow velocities to be observed. In the track filtering, the criterion of the minimum number of frames across which the features have to be traceable also causes a constraint on measurable flow velocities and camera frequencies. Again the users should be aware of these implications and guided towards a sound selection.

- Thank you for the comment. Indeed, the thresholds need to be set corresponding to the characteristic of each field site. We mentioned this in the revised manuscript. However, each threshold can be set by the user within in the provided tool and we give a guidance in the corresponding tool manual how the change of the thresholds influences the data processing. As the revised manuscript focuses in general more strongly at the tool, we also added some more details regarding the threshold choices from the tutorial to the revised manuscript.

- Indeed, an automatic selection of thresholds should be developed. However, this is on-going research and not focus of our study. But of course this is the way forward for instance considering machine learning approaches and observations of the river flow during different seasons.
- The search areas are defined automatically within the workflow if a 3D model and the water level is provided. However, the search area can also be provided to the tool using a mask image. However, we are afraid that we do not understand how the search area definition influences the admissible frequencies. The search area is set once for one observation period (over several seconds assuming a stable water level, which would be needed anyway for reliable discharge calculation) and the image area within the mask is processed for all the frames afterwards, actually decreasing processing time as only the area of interest is processed.
- The minimum number of frames to track can be set to 0 and therefore the constraints regarding flow velocities and camera frequencies are obsolete. We clarified this in the revised manuscript to avoid confusion in this regard.

7. The velocimetry procedure involved multiple filtering of particles and trajectories. This may be inefficient as compared to alternative approaches that perform the filtering only once. However, nothing is mentioned on the efficiency of the procedure. What are computational times related to image frequency and resolution? In several instances the Authors recommend to capture adequately long videos. Nonetheless, this can be time consuming and introduce additional variability due, for instance, to the occurrence of unevenly spaced tracers.

- Thank you for your note. The filtering only happens during two stages, once when features are detected, which therefore happens frequently, but this filtering is very fast. And data is filtered a second time after all features where tracked, which takes longer in processing depending on the number of detected frames but therefore this filtering is only performed once (as in alternative approaches). We provided some more guidance regarding the computational time for filtering considering frame rate and image resolution in the revised manuscript.
- Indeed, taking longer videos takes more time. But we do not think if a video is captured for 3 seconds or 20 seconds is not such a big impediment in regard of consuming time. And considering increased temporal measurement, the increase in observation length is actually beneficial for the cases of unevenly spaced tracers because chances are increased that features will eventually flow across the entire cross-section if the video is captured long enough.

8. Transformation of trajectories to rasterized cells is not clear.

- Thank you for your comment. We do not use the rasterized data for analysis and reference comparison. It is solely applied to rasterize the data. We chose a grid with a cell size of 20 pixels and interpolated the trajectories into this grid. However, in the revised manuscript we removed this figure.

9. How was the velocity coefficient estimated? This is generally an approximate methodology that is not adequate in case of irregular sections. Since water level is an input to the procedure and the bathymetry of the stream reach is reconstructed, why weren't alternative approaches be considered and integrated for flow discharge computation?

- The velocity coefficients were estimated from the ADCP measurements (as mentioned on p9, line 9). To be more specific, the velocity coefficient was estimated dividing the mean velocity of the cross section with the average surface velocity. In our study, we used a method for discharge calculation, which is commonly applied for measurement systems relying on surface velocities. Furthermore, we aimed for a direct comparison of the ADCP measurements with the variables measurable by image-based approaches. However, we agree that alternative approaches like hydraulic approaches could be useful and worth to be investigated. But we believe that this is a separate topic. It is beyond the focus of this technical note and

should be explored in more detail in further studies as research in this regard is still sparse. We addressed this in the discussion.

10. Figures should be improved. For instance, in Fig.1 panels a and b are misplaced. Also, it would be nice, for each case study, to overlap the field of view captured by each camera to facilitate velocity comparison (same difficulty in Fig.9). In Fig.3a, all points are colored, it is unclear what the Authors are referring to. In Figs. 3 and 4 it would be nice to see the influence of the various steps of the filtering. In Fig.7, points that are far from the center of images do not necessarily display higher standard deviation. This should be commented and motivated in the manuscript.

- Regarding fig. 1, we would like to mention that the panels are indeed correct; a corresponds to the Wesenitz and b to the Freiberger Mulde.
- In the revised manuscript we added the field of view of the cameras in figure 1 and the location of the ADCP measurements to figure 8 and 9 (7 and 8 in the revised manuscript).
- In fig. 3a points above the water surface are coloured with RGB information from the imagery and points under the water surface are all plotted in white. To clarify which points are meant, we differentiated between 'colorized according to their object colour' and 'white points' in the revised caption.
- Regarding the different processing step, we added further sub-figures to the show the results of the single steps of filtering.
- We are afraid that we are not able to assess why points further from the centre should reveal higher standard deviations regarding the image co-registration.

11. It would be nice to see the tracks that fall within 1 m from the ADCP measurements in a figure. In some cases, the computation is done on a very different number of trajectories regardless of the cluster-based filtering. Were values in Table 3 weighed by the number of track counts?

- We added this information in figure 7 and 8 in the revised manuscript to allow for a better assessment of the data comparison. Different numbers of trajectories are compared because each camera provided a different number of measured tracks (table 2); also after cluster-based filtering, which is a local filter, because the original density of features was already different as each camera was observing the river from a different perspective and with different camera geometry. This is mentioned in the manuscript.
- No the values were not weighted by track counts. The number of track counts represents the sample size of the statistics.

12. Even if the manuscript is mostly well readable, several typos and sentences should be improved. Some units are wrong. The sentence at lines 4 to 6 on page 7 is unclear.

- Thank you for your comment. We read and corrected the revised manuscript carefully to correct false units and remove typos.
- We rephrased the sentence lines 4-6 the following: Since most feature detectors look for regions with high contrast, points of interest would be found on the land, where contrast is usually higher than on the water surface. Thus, the river area has to be detected in the images and defined as the search area for tracking.

Some hints regarding author's changes in the revised manuscript have already been given in the comments section.

Here, a summary of author's changes to the manuscript based on comments of both referees is given.

- Focus stronger on the tool itself and its usage, thus be more specific regarding the tool (keep information about each processing stage not just in the tutorial).
- In general, explain more detailed how setting of thresholds influence tracking result and what parameters should be considered depending on the flow characteristics at different sites.
- More detailed explanation regarding the individual thresholds for track filtering.
- More detailed explanation regarding the parameter choices for feature detection and tracking (i.e. detection every nth feature and tracking for n number of features).
- More guidance regarding computational time for filtering considering frame rate and image resolution.
- Explain in more detail limits/constraints (e.g. wind, shore visibility, …), pre-requisites/ needed input (e.g. camera orientation/position or GCPs, …), and expectable results of the tool.
- Explanation of the limits for the image-based to ADCP based velocity comparison due to the accuracy of the position estimation of the ADCP.
- Clarification of the threshold (multiplying factor) definition of the statistical outlier filter.
- Clarification of the ADCP extrapolation.
- Add in figure 1 image area extents of each camera.
- Addition of sub-figures (in fig. 5) that show the results of the different feature track filtering steps.
- Removal of the figures with the rasterized velocities (fig. 8 and 9) and instead add figure with the final tracks. In addition, add to this figure location of ADCP cross-section(s).
- Improve the readability of the manuscript.
- Include an appendix with information about accuracies for estimation of exterior camera geometry. Furthermore, we had to correct the s0 values in Table 2 because in the Discussion paper we accidently used a false pixel size (from the still image format instead of the frame format) to calculate s0 (it is originally correctly given in mm in the software, but we transformed it to pixel values for better assessment).
- Include an appendix with information about the chosen parameters within the FlowVelo tool to perform velocity estimations with all camera variations.
- Provide the manual of the tool as a separate supplement (in addition to the huge supplemental zip-file)

Flow velocity and discharge measurement in rivers using terrestrial and UAV imagery

Anette Eltner[1], Hannes Sardemann[1], Jens Grundmann[2]

[1]Institute of Photogrammetry and Remote Sensing, Technsiche Universität Dresden, Dresden, 01069, Germany
[2]Institute of Hydrology, Technsiche Universität Dresden, Dresden, 01069, Germany

Correspondence to: Anette Eltner (anette.eltner@tu-dresden.de)

Abstract. An automatic workflow to measure surface flow velocities in rivers is introduced, including a Python tool. The method is based on PTV and comprises an automatic definition of the search area for particles to track. Tracking is performed in the original images. Only the final tracks are geo-referenced, intersecting the image observations with water surface in object space. Detected particles and corresponding feature tracks are filtered considering particle and flow characteristics to mitigate the impact of sun glare and outliers. The method can be applied to different perspectives, including terrestrial and aerial (i.e. UAV) imagery. To account for camera movements images can be co-registered in an automatic approach. In addition to velocity estimates, discharge is calculated using the surface velocities and wetted cross-section derived from surface models computed with structure-from-motion and multi-media photogrammetry. The workflow is tested at two river reaches (paved and natural) in Germany. Reference data is provided by ADCP measurements. At the paved river reach highest deviations of flow velocity and discharge reach 4 % and 5 %, respectively. At the natural river highest deviations are larger (up to 31 %) due to the irregular cross-section shapes hindering accurate contrasting of ADCP- and image-based results. The provided tool enables the measurement of surface flow velocities independently of the perspective from which images are acquired. With the contact-less measurement spatially distributed velocity fields can be estimated and river discharge in previously ungauged and unmeasured regions can be calculated, solely requiring some scaling information.

1 Introduction

Measuring discharge of rivers is a major task in hydrometry because of its importance in many hydrological and geomorphological research questions, e.g. to understand the characteristics of catchments and their adaption to climatic changes. Different approaches exist to apply the velocity-area-method to measure discharge relying on information about the flow velocity and the wetted river cross-section area. Established tools to retrieve flow velocities are the application of current meters, acoustic devices (i.e. acoustic Doppler current profilers) or surface velocity radar (Herschy, 2008, Merz, 2010, Morgenschweis, 2010, Gravelle, 2015, Welber et al. 2016). However, these velocity estimation methods are either labour intense, require minimum water depths, need prolonged measurement periods or can endanger the operator during flood measurements.

A promising alternative are remote sensing tools utilising image-based approaches. Due to their flexibility (only a camera is needed) they are used frequently exploiting various sensors and platforms for data acquisition. For instance, RGB sensors have been used (e.g. Muste et al., 2008) as well as thermal cameras (e.g. Puelo et al., 2012). Ran et al. (2016) demonstrated the suitability of a low-cost Raspberry Pi camera to observe flash floods. And Le Coz et al. (2016) and Guillén et al. (2017) illustrated the usability of crowd-sourced imagery for post-flood analysis. Image-based setups allow for the assessment of temporally changing flow dynamics (Sidorchuk et al., 2008) due to the potential continuous recording of entire river reaches. Furthermore, small-scale investigations are enabled as shown by Legout et al. (2012), who measured the spatial distribution of surface runoff from mm- to cm-depth, at a range where other methods are failing.

Various algorithms exist for surface flow velocity monitoring from image-based observations deploying tracking tools. Four tracking approaches are applied frequently in the field to monitor rivers. The first method is large scale particle image velocimetry (LSPIV) originally introduced by Fujita et al. (1998). This approach uses tracking of features at the water surface that are caused due to natural occurring floating particles or free surface deformations caused by ripples or waves e.g. due to wind or turbulences (Muste et al., 2008). In general, the area of interest (i.e. the water surface) is divided in sub-regions and these sub-regions are used as templates. In the subsequent images, the corresponding areas are searched for using correlation techniques.

Fujita et al. (2007) advanced the LSPIV approach by an algorithm called space time image velocimetry (STIV). STIV performs faster, because tracking is performed in 1D instead of 2D. Profiles are extracted along the main flow direction to subsequently draw particle movements along the time axis (i.e. change along the profiles within succeeding frames) leading to a space-time image. The resulting angle of the pattern within that image resolves into the actual flow velocity.

The third possibility is the usage of optical flow algorithms developed in the computer vision community. For instance, the Lucas-Kanade (Lucas & Kanade, 1981) operation has been utilized to measure surface velocities of large floods or small rivers (Perks et al., 2016 or Lin et al., 2019, respectively). The method aims to minimize grey scale value differences between template and search area adapting the parameters of an affine transformation within an optimization procedure.

Finally, particle tracking velocimetry (PTV) is a tracking option that uses correlation techniques as in LSPIV. However, instead of using entire sub-regions as templates single particles are detected first and then searched for in the subsequent images.

LSPIV is the most widely used method and can be considered as matured (Muste et al., 2011). Amongst others, it enabled the measurement of the hysteresis phenomena during flood events (Tsubaki et al., 2011, Muste et al., 2011). However, LSPIV mostly underestimates velocities, which is revealed in more detail by Tauro et al. (2017), who prefer PTV instead. In contrast to LSPIV it PTV does not assume similar flow conditions for the entire search area and it is not influenced by surface frictional resistance (Lewis and Rhoads, 2015) or standing waves (Tsubaki et al., 2011).

Besides surface flow velocity another parameter has to be considered to derive discharge measurements from image-based tracking approaches. The depth averaged flow velocity, used in the velocity-area-method, does not necessarily correspond to the surface flow velocity, which is amongst others due to the influence of river bed roughness. Therefore, a so called velocity

coefficient has to be used to adjust the surface velocities (Creutin et al., 2003, Le Coz et al., 2010). Usually, the deeper the flow the higher the coefficient is assumed (Le Coz et al., 2010). The coefficient can vary with different river cross-sections (Le Coz et al., 2010) and it can change within the same cross-section due to varying water ~~levels~~depths, which is likely for irregular profiles (Gunawan et al., 2012). Muste et al. (2008) state that the coefficient mostly ranges between 0.79 to 0.93, but values as low as 0.55 have been measured (Genc et al., 2015). Considering the correct velocity coefficient is important because it has a high impact on the discharge estimation error in remote sensing approaches (Dramais et al., 2011).

When flow-velocities and velocity coefficient are known, the area of the river cross-section is needed to calculate the discharge with the velocity-area method (e.g. Hauet et al., 2008). Different tools exist for contactless river cross-section area measurement. Muste et al. (2014) show that it is possible to use velocity pattern measured with LSPIV to retrieve flow depth in shallow flow conditions. Another approach is the utilization of ground penetrating radar as illustrated for larger rivers by Costa et al. (2000). An additional increasingly used method to retrieve the topographic (and thus cross-section) information of the river reach is the usage of structure-from-motion (SfM) photogrammetry (Eltner et al., 2016). For instance, Ran et al. (2016) capture stereo images to reconstruct the 3D information of a river reach from overlapping images during low flow conditions. However, if water is present during data acquisition and the river bed is still visible the underwater measurements have to be corrected for refraction impacts (Mulsow et al., 2018) or else heights of points below the water surface will be underestimated. Woodget et al. (2015) introduce a workflow to account for refraction using a constant correction value for the case of Nadir viewing image collection. Dietrich (2017) extends this correction procedure for the case of oblique imagery. Detert et al. (2017) were the first to perform fully contact-less, image-based discharge estimations using refraction corrected river cross-sections (adapting Woodget et al., 2015) and surface flow velocities, all measured from UAV imagery. However, the authors relied on a seeded flow to apply LSPIV.

Image-based tracking approaches can be applied to imagery captured terrestrially as well as from aerial platforms. In the case of aerial imagery, the utilization of UAVs for data acquisition is increasing. The advantage of drones is their flexibility and allowance to capture runoff patterns during high flow conditions (e.g. Tauro et al., 2016, Perks et al., 2016, Detert et al., 2017, Koutalakis et al., 2019), even enabling real-time data processing (Thumser et al., 2018). However, a challenge to overcome is the correction of camera movements during the UAV flight. Although camera mounts are commonly stabilised, remaining motions need to be accounted for. Tauro et al. (2016) subtract velocities measured in stable areas outside the river from velocities tracked in the river. Another possibility is the usage of co-registration. Thereby, either features (e.g. SIFT features; Lowe, 2004) are searched for in stable areas (Fujita et al., 2015, Blois et al., 2016) or Ground Control Points (GCPs) are detected (Le Boursicaud et al., 2016). Subsequently, these image points are matched across the images. Afterwards, this information is used to apply a perspective transformation to each image to fit them to a reference image. However, so far stable areas are still masked manually.

In the case of terrestrial data acquisition, the conversion of pixel measurements to metric velocity values is more challenging compared to UAV data due to a stronger deviation of the perspective from an orthogonal projection, which leads to decreasing accuracies with increasing distance to the sensor. Therefore, Kim et al. (2008) suggest to avoid camera setups

with tilting angles larger than 10°. Most approaches ortho-rectify the images prior tracking to allow for a correct scaling of the image tracks. However, performing the tracking in the original image would be favoured to minimize interpolation errors, especially for oblique camera setups, and to solely transform the tracked image point coordinates into object space (Stumpf et al., 2015).

Several software tools already exist to perform image-based velocimetry (e.g. PTVlab from Brevis et al. 2011, PIVlab from Thielicke & Stamhuis 2014, Fudaa-LSPIV at https://forge.irstea.fr/projects/fudaa-lspiv, KU-STIV developed by Fujita, or RIVeR from Patalano et al. 2017). These tools cover different processing steps and tracking options to retrieve surface flow velocities and discharge. In this study, we combine the entire workflow from video, either captured with UAV or from terrestrial camera, to velocity of river reaches, considering image stabilization, automatic feature search area extraction, PTV, track filtering and metric velocity retrieval via forward ray intersection.

~~In this study, a~~An automatic flow velocity measurement tool (FlowVelo ~~T~~tool) for image velocimetry is presented~~. The FlowVeloTool~~ and ~~is~~ provided by public domain ~~and~~ to overcome~~s~~ existing gaps discussed before. It is independent from the data acquisition scheme and relies on PTV. Camera movements are accounted for in a fully automatic approach if a sufficient amount of shore area is visible. Furthermore, the search area for features to track, i.e. the river area, is extracted automatically solely requiring water level information and a 3D surface model of the river reach. The 3D surface model is calculated from image data with SfM photogrammetry additionally considering multi-media photogrammetry to retrieve both, topography and bathymetry. In order to improve tracking results, detected features and velocity tracks are filtered with different methods. Finally, we estimate discharge from surface flow velocities and cross sectional areas. The FlowVelo ~~Tool~~ tool and the whole workflow are investigated for two river reaches, paved and natural, at which velocities and discharges are compared to ADCP references.

2 Methods

In this study, the FlowVelo ~~T~~tool is introduced that allows for the measurement of flow velocity from videos independently from the acquisition platform, i.e. either aerial or terrestrial. Different parameter options for feature detection and tracking as well as track filtering are explained. Two experimental study sites have been chosen to evaluate the performance of video based flow velocity estimation using camera frames acquired from different perspectives. First the experimental study sites are introduced and afterwards the tool is explained.

2.1 Areas of interest

The experimental study sites are short river reaches in Saxony, Germany (fig. 1). One studied river reach is situated at the Wesenitz. This river originates in the Lausitzer highlands, has a catchment size of about 280 km², and exhibits a river length of 83 km. The area of interest is located at the river gauge station Elbersdorf, which is operated by the Saxon state company for environment and agriculture. Here, annual average water level and discharge for the hydrological year 2017 are 48 cm

and 2.~~2~~ 4 m²/s, respectively. Field campaigns were conducted on March 31st and on April 4th 2017. During the campaigns water level amounted 51 cm (discharge 2.7 m³/s). The investigated river section at the Wesenitz is paved but influenced by local sand banks at the river bottom. During the data acquisition the river had a width of about 10 m.

The other river is the Freiberger Mulde, which originates in the Ore Mountains, has a catchment size of about 2980 km², and displays a river length of 124 km. The area of interest is located close the gauge Nossen. Average discharge and water level for the hydrological year 2016 are ~~6.9~~5.6 m³/s and ~~66~~ 65 cm, respectively. The gauge station is located 1 km upstream of the studied river reach. The field campaign was conducted on October, 26th 2016. During this day discharge and water level were 5.7 m³/s and 68 cm. The approximated river width was 15 m. The chosen region of interest at the Freiberger Mulde is a natural river section with non-uniform flow conditions.

2.2 Data acquisition

Different data was collected during the field campaigns at both river sections. Amongst others ADCP measurements were performed as flow velocity reference, GCPs were defined to geo-reference the video data and UAV and terrestrial imagery were acquired to perform image-based flow velocity estimation.

2.2.1 ADCP measurements

For the ADCP measurements the moving boat approach with StreamPro from RDI is used. Velocity profiles were measured with a blanking range of 14 cm near the water surface. Data were processed using the AGILA software from the German Federal Institute of Hydrology (BfG). Measurements along the boat track were projected onto a reference cross sectional area. Afterwards surface flow velocities were extrapolated to allow for a comparison to the image-based values. For the extrapolation, power functions were fitted to the measured vertical velocity profile for each individual ADCP ensemble using the software AGILA (for more detail see Adler, 1993 and Morgenschweis, 2010). Then, velocities at the water surface were calculated with these functions. Thus, all ADCP measurements of the profile were considered to extrapolate surface velocities.

At the Wesenitz ADCP measurements were performed at one cross-section in eight repetitions (fig. 1a). Average water surface velocity was about 0.7 m/s and resulting discharge amounts 2.7 m³/s (table 1). At the Freiberger Mulde three cross-sections were chosen (fig. 1b) to acquire data that allows for a spatially distributed assessment of the image-based data. Average river surface velocities ranged between 0.60 m/s and 0.76 m/s (table 1).

The spatial variation of flow velocities is larger at the Freiberger Mulde, where measurements were performed in a natural river reach, which is in contrast to the flow velocity range at the Wesenitz, where data was captured at a standardized gauge station. Thus, only one profile was measured at the Wesenitz. The discharge at the Freiberger Mulde is 5.88 m³/s on average but reveals a standard deviation of 0.25 m³/s. Estimated discharge of the river reach therefore reveals a variation of about 4 %, which can be attributed to inconsistencies during data acquisition. A decrease of the velocity coefficient, which has

been derived from the ADCP measurements, with decreasing water depth is observed. At the Freiberger Mulde cross-sections 1 and 3 (Table 1) have lower water depth compared to profile 2. Thus, the velocity coefficients are lower.

2.2.2 Image-based data

At both river reaches video sequences were acquired with terrestrial cameras and with a camera installed at the UAV Asctec Falcon 8. The airborne image data was captured at flying heights of about 20 m and 30 m at the Wesenitz and Freiberger Mulde, respectively. Videos were captured with a frame rate of 25 frames per second (fps) and with a resolution of 1920 x 1080 pixels using the camera Sony NEX-5N with a fixed lens with a focal length of 16 mm. The ground sampling distance (GSD) is about 7 mm at the Wesenitz and about 9 mm at the Freiberger Mulde.

The terrestrial cameras were installed at bridges across the river (fig. 1). At the Wesenitz three cameras were installed to evaluate the performance of different cameras (fig. 1a). Two Canon EOS 1200D and one Canon EOS 500D were setup. The 1200D cameras captured video sequences with 25 fps and with a resolution of 1920 x 1080 pixels. The 500D captured frames with a higher rate (30 fps) and smaller image resolution (1280 x 720 pixels). All three cameras were facing downstream. At the Freiberger Mulde the camera Casio EX-F1, equipped with a zoom lens fixed to 7.5 mm, was used. Videos were captured with 30 fps and a resolution of 640 x 480 pixels. The camera was facing upstream.

The terrestrial cameras were calibrated for both rivers to allow for the correction of image distortion impacts. To estimate the interior geometry of the cameras, images of an in-house calibration field have been captured in a specific calibration pattern (Luhmann et al., 2014). These images, together with approximate coordinates of the calibration field and approximations of the interior camera orientations were used in a free-network bundle adjustment within Aicon 3D Studio to calibrate each camera. More details regarding the workflow are given in Eltner et al. (2015).

2.3 High resolution topography of the river reaches

Local 3D surface models describing the topography of the river reaches are necessary to scale the image measurements. Therefore, high resolution topography data was acquired at both rivers using SfM photogrammetry (Eltner et al., 2016, James et al., 2019). SfM in combination with multi-view stereo matching (MVS) allows for the digital reconstruction of the topography from overlapping images and some GCPs. Thereby, homologous image points in overlapping images are detected and matched automatically. From these homologous points and some assumptions about the interior camera model, the position and orientation of each captured image (i.e. camera pose) can be calculated. With known network geometry, a dense point cloud can be computed, reconstructing the 3D information for almost each image pixel. The resulting 3D surface models are geo-referenced during the reconstruction or afterwards via GCPs.

At the Wesenitz the 3D surface model of the river reach was calculated from 85 terrestrially captured images with a Canon EOS 600D (20 mm fixe lens) and from 20 UAV images (Eltner et al., 2018). The SfM calculations were performed in Agisoft Metashape. At the Freiberger Mulde seven frames of the video sequence, which is also used for later PTV processing, were utilized to perform SfM photogrammetry to retrieve the corresponding 3D model of the river reach.

GCPs made of white circles on a black background were installed in order to reference the 3D data as well as the image-based velocity measurements. They were measured with a total station at the Freiberger Mulde and during the first campaign at the Wesenitz. During the second campaign at the Wesenitz GCPs were extracted from cobblestone corners (with sufficient contrast) at the gauge, which are visible in the terrestrial images used for the 3D model reconstruction. GCPs were measured in at least five images for sufficient redundancy and thus more reliable coordinate calculation.

The bathymetric information of the river reaches was retrieved using the same UAV data as for the topographic information above the water level. Refraction impacts are accounted for using the tool provided by Dietrich (2017). Underwater points, camera poses and interior camera parameters as well as the water level need to be provided. The corrected point clouds can be noisy and were therefore filtered and smoothed in CloudCompare using a statistical outlier filter to detect isolated points and using a moving least square filter. Eltner et al. (2018) revealed that cm-accuracies can be reached using multi-media SfM at the Wesenitz river reach.

2.4 Surface Flow Velocity Workflow – the FlowVelo ~~T~~tool

This chapter introduces the general approach to measure surface flow velocities from either terrestrial or airborne video sequences. Thereby, essential processing steps are described in more detail. The FlowVelo ~~T~~tool is realized in Python and using the OpenCV library (Bradski, 2000). Fig. 2 illustrates the entire data processing workflow of the tool.

2.4.1 Frame preparation

Video sequences are converted into individual frames prior to the data processing. Afterwards, image co-registration is necessary if the camera is not stable during video capturing, as it is the case for the UAV data. Each frame of the entire video sequence is co-registered to the first frame of the same sequence to correct camera movements and thus to enable that all frames capture the same scene. This processing step is preformed fully automatically. In each frame Harris corner features are detected (Harris & Stephens, 1988), which are then matched to the first frame of the sequence using SIFT ~~descriptors~~ (Lowe, 2004) or ORB descriptors (Rublee et al., 2011). The suitability of co-registration in different conditions and over longer periods of time has been illustrated in Eltner et al. (2018), who introduce a terrestrial camera gauge for water level measurements.

Harris features in the water region are detected as outliers due to their changing appearance between subsequent frames leading to matching failure. And if moving features in the water area still might be matched, they are latest filtered during the parameter estimation of the homography because these points will be considered as outliers during the model fitting with RANSAC (Fischler & Bolles, 1981). Thus, only stable and reliable homologous image points outside the river are kept and used to calculate the homography parameters between the first frame and all subsequent frames. Finally, a perspective transformation is applied to ensure that all frames fit to the first image. It has to be mentioned that this approach is only working as long as enough stable areas are visible on both river shores.

In the FlowVelo tool five parameters can be set to adjust the co-registration of each individual scenery. The maximum number of keypoints defines how many features are maximally searched for in each frame. Larger numbers can increase the robustness and accuracy of matching but also the processing time. The number of good matches determines how many matched features between two frames are needed minimally to find the homography. Again, larger values increase the robustness, but they can also lead to a failure of processing if fewer feature matches are found than appointed here. Furthermore, it can be defined, which feature descriptor is chosen for matching, if features are matched back and forth increasing the accuracy and processing time, and if image co-registration is performed to the first frame or in a series to each consequent frame of the sequence.

2.4.2 Finding features to track

A search area in the river region has to be defined to detect particles before tracking. This is due to the circumstance that most feature detectors look for regions with high contrast. Therefore, points of interest would be found on the land, where contrast is usually higher than on the water surface. Thus, in a first step the river area has to be masked in the images and defined as the search area for tracking before applying particle detection ~~within the entire image will lead to the detection of points of interest in regions with more contrast outside the water area as most feature detectors are looking for regions with high contrast. Thus, the water area needs to be masked in a first processing step~~.

Feature search area and pose estimation

The feature search area is a region of interest that is defined as a function of the water level to mask the image. The water level and a 3D surface model of the river reach (fig. 3a) observed by the camera have to be known to define this water area automatically. The 3D surface model is clipped with the water level value to keep solely the points below the water surface. Afterwards, these points are projected into image space (fig. 3b). Therefore, information about the pose and the interior geometry of the camera is necessary. In the FlowVelo tool information about the camera pose is either estimated with spatial resection considering the GCP coordinates in image and object space and the interior camera parameters (for more details see Eltner et al., 2018) or it can be simply stated if the pose has been defined by other measures.

Next, ~~T~~the 3D point cloud of the observed river reach is projected into a 2D image (fig. 3b). To fill gaps, potentially arising for 3D surface models with low resolution, a morphological closing is performed. Finally, the contour of the underwater area is extracted to define the search mask for the individual frames. If several contours are detected, the largest contour is chosen. If a 3D surface model is not present for automatic feature search area detection, the area of interest for tracking can also be provided via a mask file.

Feature detection and filtering

Particles are detected with the Shi-Tomasi feature (or good feature to track; GFTT) detector (Shi & Tomasi, 1994). Thereby, features are detected similar to the Harris corner detector but a different score is considered to decide for a valid feature (fig. 3c). Many more feature detectors are possible. Tauro et al. (2018) test several methods and show that the GFTT detector performs well and also finds features in regions of poor contrast.

The elimination of particles, which are not suitable for tracking, is necessary. For instance, reflections of sunlight at waves showing high contrasts on the water surface need to be removed to avoid erroneous tracking of fake particles (Lewis and Rhoads, 2015). Therefore, a nearest neighbour search is performed to find areas with strong clusters of particles. If there are too many features within a defined search radius, the particle will be excluded from further analysis. In addition, features are removed that reveal brightness values below a threshold, e.g. to avoid the inclusion of wave shadows as features.

2.4.3 Feature tracking

When features have been detected, they are tracked through subsequent frames (fig. 4). This tracking is performed using normalised cross correlation (NCC). Normalization allows accounting for brightness and illumination differences between different frames. The positions of the detected features are chosen to define templates with a specific kernel size (mostly 10 pixels in this study, Appendix 2). In the next frame NCC is performed within a defined search area (mostly 15 pixels in this study, Appendix 2) to find the positions with highest correlation scores for each feature, potentially corresponding to the new positions on the water surface of the migrated particles.

To refine the matching, an additional subpixel accurate processing is performed. Thereby, template and matched search area of the same size are converted into the frequency domain to measure the phase shift between both and afterwards the subpixel peak location it determined with a weighted centroid fit. The final matched locations define the new templates for tracking in the next frame. This tracking approach is performed for a specified number of frames. In this study, features are tracked for 20 frames and new features are detected every 15th frame. It can be suitable to detect features more frequently than the number of frames they are tracked across, because features can change their appearance and new features can enter the area of view although the already detected features are still tracked.

2.4.4 Track filtering

Figure 4 shows that false tracking results can still occur, e.g. tracks that significantly deviate from the main flow direction. This is amongst others due to remaining speckle detected as features or due to tracking of features with low contrast leading to ambiguous matching scores. Therefore, resulting velocity tracks need to be filtered. Tauro et al. (2018) remove false trajectories considering minimum track length and track orientation. In this study, we also make ~~four~~ assumptions about the flow characteristics of the river (fig. 5). We consider six parameters; minimum frame amount of a tracked feature, minimum and maximum tracking distances, flow steadiness, range of track directions, and deviation from average flow direction.~~Thereby, e~~ Each track has to fulfil these criteria to be considered as a reliable velocity information. Thereby, each track is the combination of the individual sub-tracks from frame to frame, with feature detection performed in the first frame. The ~~second~~first criterion considers the minimum ~~number~~percentage of frames across which the features have to be traceable (here ~~13~~65 % ~~frames~~).The underlying assumption is that if the feature is only traceable across a few frames then it is more likely not a well-defined flowing particle at the water surface but may for instance be a speckle occurrence due to sun glare. However, the minimum value can be set to 0 to avoid any constraints regarding flow velocities and camera frame rates.

The ~~first~~ second and third filter ~~criterion~~ criteria ~~is~~ are the distances across which features were tracked, comprising thresholds for minimum and maximum distances. The distance thresholds can be roughly approximated when image scale and the range of expected river flow velocity is known. In this study, the minimum and maximum distance parameters are set to ~~zero~~ 0.1 and ~~ten~~ 10 pixels, respectively. ~~The second criterion considers the minimum number of frames across which the features have to be traceable (here 13 frames).~~

The ~~third and~~ fourth criterion~~s~~ considers ~~parameters of~~ the directional flow ~~direction~~behaviour of the feature~~. On the one hand, the~~ with a steadiness ~~of the flow behaviour is analysed~~parameter. Therefore, directions of sub-tracks (from frame to frame) are analysed for each track. Tracks are excluded when the standard deviation is above a defined threshold (30° in this study). The idea is that river observations are performed during nearly ~~steady~~uniform flow conditions. Thus, high frequencies of changes in flow directions within a track indicate measurement errors and should be filtered. In addition to this steadiness parameter, the range of all sub-track directions is also considered as a measure of the flow behaviour. If~~or~~ the range ~~of these sub-track directions are~~is above a defined thresholds the track will be excluded (here ~~30° and~~ 120°~~, respectively~~).

~~On the other hand~~For the last criterion~~,~~ the main flow direction of the river is examined. ~~by calculating t~~The average direction of all tracks is calculated and~~. I~~if the direction of ~~one~~ the individual tracks ~~is~~ are larger or below a buffer threshold (here 30°), ~~it~~ they ar~~is~~e rejected ~~for~~ from further processing. The buffer value has to be defined considering the general variability of the river surface flow pattern. The lower the parameter is chosen the more a uniform flow is assumed. It has to be noted that the directional filter has a limited applicability in more complex flow conditions, e.g. turbulent, non-uniform rivers. In such situation, local filters should be preferred over these global values.

2.4.5 Velocity retrieval

In the last processing stage, measured distances are transformed from pixel values to metric units to receive flow velocities in the unit of m/s. With known camera pose and interior camera geometry image measurements can be projected into object space. This leads to a 3D representation of the light ray emerging from the image plane and proceeding through the camera's projection centre. 3D object coordinates of an image measurement can be calculated by intersecting its ray with a 3D surface model of the river. In this case the water surface, assumed as planar at the water level, defines the location of intersection. The starting and ending points of each track are intersected with the water plane to retrieve real world coordinates. From the distance between start and end, and considering the camera's frame rate as well as the number of tracked frames, metric flow velocities are retrieved.

Finally, the metric velocity tracks are filtered once more with a statistical outlier filter to remove remaining outliers (fig. 6). The threshold is defined as the sum of the average velocity with a multiple of its standard deviation (e.g. Thielicke & Stamhuis, 2014). The lower the multiple is chosen, the more features will be filtered and only tracks will be kept, which have

values close to the average velocity. In this study, the parameter was set to 1.5. This processing step is more important for challenging tracking situations. ~~For a better visualisation, final flow velocity tracks are rasterized.~~

Regarding tracking reliability, it should be noted that in the case of terrestrial cameras with an oblique view onto the river velocity measurements are preferred closer to the sensor. Particles move across a larger number of pixels in close range to the camera than in further distances, e.g. an erroneous measurement of 1 pixel close to the camera might result to measurement error of 1 cm whereas in further distance it can correspond to 1 m. Furthermore, tracking accuracy decreases significantly in far ranges due to increasing glancing ray intersections with the water surface.

2.5 Discharge estimation

The bathymetric information as well as the flow velocities are needed to calculate the discharge. Thereby, sole UAV data can be used as shown by Detert et al. (2017). In this study, we cut river cross-sections from the reconstructed bathymetry and topography at the approximate locations of the ADCP measurements. Afterwards, we extract the water level information by manually detecting the water line in at least three overlapping images and spatially intersecting these point measurements in the object space.

The surface flow velocity values are averaged and multiplied with the velocity coefficients estimated from the ADCP measurements to account for depth-averaged velocities (Table 1). This approach is suitable at the Wesenitz. But at the Freiberger Mulde the method is restricted due to the irregular river cross-sections limiting the application of a constant velocity coefficient. Finally, discharge is estimated by multiplying the cross-section area with the depth-averaged velocity.

3 Results and Discussion

In this chapter, results of the accuracies of the image processing are displayed, tracked flow velocities are evaluated, and discharge estimations are analysed.

3.1 Accuracy assessment of camera pose estimation and image co-registration

To enable an accurate measurement of flow velocities it is necessary to consider how well the camera pose has been estimated. Furthermore, for cameras in motion the accuracy of frame co-registration has to be evaluated as well, to ensure that tracked movements of the particles indeed correspond to river flow instead of camera movements.

The accuracy of camera pose estimation can be estimated because more than three GCPs are available. In general, the camera pose will be calculated more accurately if GCPs are distributed around the area of interest in the object space and if images capture them in such a way that they cover the entire image extent because it allows for a stable image-to-object geometry. Furthermore, for highest accuracy demands GCPs need to be measured with high accuracy in object space and ideally with sub-pixel accuracy in image space. At both river reaches accuracies are better for the terrestrial cameras (table 2), which is due to a higher GSD as cameras are significantly closer to the area of interest compared to the UAV

cameras. At the Wesenitz, another reason for the larger deviations is the circumstance that well marked, artificial GCPs were used for the terrestrial images, whereas GCPs were extracted from the 3D surface models to estimate the UAV camera pose leading to lower point coordinate accuracies.

Small template regions (10 pixels in size) in stable areas have been chosen (fig. ~~7~~6) to estimate the accuracy of frame co-registration. At the Freiberger Mulde only GCPs could be used as templates because the remaining area of interest is covered by vegetation that changes frequently. At the Wesenitz cobble stone corners close to the river surface are chosen because it is important to see how well co-registration performs close to the water body for which velocities are estimated. Each extracted reference location is tracked through the frame sequence via NCC. In case of a perfect alignment, the templates should remain at the same image location throughout the sequence. In this study, at the Freiberger Mulde average deviation between tracked frames to the first frame amounts 0.5 ± 0.6 pixels for all templates, which corresponds to a co-registration accuracy of 4.3 ± 5.2 mm. At the Wesenitz, co-registration reveals an accuracy of 1.0 ± 1.6 pixels (6.8 ± 11.3 mm). The lower image coverage of the right shore at the Wesenitz leads to a lower quality of the frame co-registration when compared to the Freiberger Mulde reach because features for frame matching are only kept outside the water area as the appearance of the river surface changes too quickly. Therefore, higher deviations are measured at the right shore than at the left shore. Considering only the matched targets at the left river side reveals an error range similar to the Freiberger Mulde.

3.2 Flow velocity measurements at the Wesenitz

The tracking results and retrieved flow velocities show a diverse picture for the different cameras. For instance, the final number of flow velocity tracks is different for each device (table 2). The lowest number of tracks is measured for the UAV camera. However, this camera solely captured a very short video sequence (about three seconds) that could be used for tracking. Furthermore, GSD of the UAV data is much lower than the GSD of the terrestrial cameras due to a larger sensor to object distance. The terrestrial cameras reveal a significantly denser field of flow velocity tracks (fig. ~~8~~7). The terrestrial cameras captured videos of a length of about half a minute. Although video lengths of the terrestrial cameras are similar, the number of final velocity tracks is varying. The camera closest to the water surface and with the least oblique view (1200D-II) reveals the highest track number. Camera 1200D-I reveals a lower number of velocity measurements, although frame resolution and focal length are the same and video length is even longer. The third camera (500D) depicts lowest track number, which is mainly due to a lower frame resolution.

Besides considerations of the camera geometry, track filtering is another very important aspect to retrieve reliable velocity measurements. The filtered track number is about a magnitude lower than the raw track amount for the terrestrial cameras (table 2) highlighting the importance of video sequences with sufficient temporal duration. Thus, tracking should be performed as long as possible to increase the robustness of velocity filtering.

Comparing the range of flow velocity values between the different terrestrial cameras and the UAV camera reveals a good fit (fig. ~~8~~7), which also coincides with the ADCP reference (table 3). Furthermore, regions of faster and slower velocities are revealed in the terrestrial image data that also show within the acoustic data. The average deviation of all

cameras to the ADCP measurements are calculated for video-based track values that are within a maximal perpendicular distance to the ADCP profile of 1 m. The difference amounts to 0.03 ± 0.06 m/s. However, it is difficult to perform exact comparison to the ADCP measurements because the precise location of the ADCP cross-section in the local coordinate system of the river reach is not known as the ADCP boat was not equipped with any positioning tool and its movement across the water surface was neither tracked nor synchronised. Therefore, accuracy assessment of the spatial velocity pattern is limited. Nevertheless, we were able to identify the start and end points of the cross-sections at the shore in the imagery. Therefore, we could approximately estimate the locations of the cross-sections in the decimetre range, which allows for velocity comparison if the surface flow velocity pattern does not become too variable within shortest distances. This has to be kept in mind, when assessing the velocity differences, especially at the Freiberger Mulde.

Average surface flow velocities from the image-based measurements are higher or similar to the (extrapolated) ADCP retrieved surface velocity of 0.7 m/s, except for camera 1200D-II, which depicts lower values; also compared to the other cameras (table 4). A potential reason is the different coverage of the cross-section with measured velocity values. 1200D-II reveals the highest velocity value density and covers a larger part of the cross-section (fig. ~~8~~7). More regions with lower velocities are measured by the 1200D-II, whereas the other cameras feature less cross-section coverage and more values are measured in areas of faster velocities.

Interestingly, an impact of the missing camera calibration of the UAV images is not obvious. Lens distortion parameters were only modelled for the terrestrial cameras but were discarded for the UAV camera. The impact is assumed to be minimal because the camera distortion is usually especially large for cameras with very wide angles, which is not the case for the UAV camera. Furthermore, the distortion impact is more important when features are tracked for large distances in the image, which is also not the case in this study because features are mostly tracked between subsequent frames for only a few pixels.

3.3 Flow velocity measurements at the Freiberger Mulde

At the Freiberger Mulde a more diverse spatial velocity pattern becomes obvious (fig. 8). Especially the UAV data reveals areas of increased and decreased velocities along the river reach. Velocity ranges coincide with the ADCP measurements. Average deviations of the closest tracks to the reference values (similar approach to chapter 3.2) are on average 0.01 ± 0.07 m/s for the terrestrial and UAV camera and for all cross-sections. However, velocities are either overestimated or underestimated at different profiles and for different cameras (table 3). The flow velocities for the UAV data is lower at profile 3 compared to the reference. However, due to the strong changes of flow velocities within short distances, especially at cross-section 3 (fig. 1), a possible reason can be false mapping of ADCP values to image-based values. ~~This~~ The assumption that velocity underestimation at that cross-section is due to imprecise point-based velocity comparison is backed when comparing the average cross-section UAV-retrieved surface velocity (table 4) with the average ADCP velocity. In ~~this~~ that case, the UAV data reveals larger values (0.79 versus 0.76 m/s, respectively), confirming the observations at cross-section 1 and 2.

The terrestrial camera depicts a lower spatial density of velocities compared to the terrestrial cameras at the Wesenitz (table 2), although the video sequence has comparable length. This is due to the significantly lower image resolution as well as the larger distance to the object. Therefore, less features are detectable. The average flow velocity at cross-section 1 as well as the average of contrasted individual velocity tracks are smaller than the reference. However, error behaviour of the image-based data might be less favourable at cross-section 1, where the comparison is made for image tracks measured at the far reach of the image. The sharp glancing angles at the water surface lead to higher uncertainties of the corresponding 3D coordinate.

The decision about how to set the parameters for tracking (e.g. patch size) and filtering (e.g. statistical threshold) remains challenging, especially in long-term applications when spatio-temporal flow conditions can change strongly (Hauet et al., 2008). Thus, in future studies intelligent decision approaches for corresponding parameters need to be developed, for instance where measurements are performed iteratively with changing parameters.

3.4 Camera based discharge retrieval

Discharge estimations at the Wesenitz do not show large deviations between the cameras because velocity estimates showed low deviations, as well (table 4). Solely camera 1200D-II displays a lower discharge. Average discharge for all cameras amounts to 2.7 m³/s, which corresponds to the ~~velocity~~ discharge measured by the ADCP. Deviations to the reference are below 4 %, highlighting the great potential of UAV application to retrieve discharge estimates solely from image data in regular river cross-sections. Standard deviations of the discharge estimations due to the consideration of the standard deviation of the surface flow velocities is small, ranging from 0.18 m³/s (7 %) to 0.56 m³/s (8 %) at the Wesenitz and Freiberger Mulde, respectively (table 4).

At the Freiberger Mulde, discharge estimates do not fit as well to the reference measurements. Velocities are only observed in the main flow of the river, where flow velocities are higher. Deviations to the ADCP reference are larger for the terrestrial camera, whose measurements are only compared to profile 1, which shows the largest range of flow velocity and depicts very low values outside the main flow (fig. 1). Comparing single velocity values to nearby ADCP measurements, instead of averaged cross-section information, reveals that the accuracies of image-based velocity measurements are indeed higher (table 3). Neglecting the slower flow velocities in the shallower river region outside the main flow leads to overestimated discharge values for the irregular shaped cross-sections, which is in contrast to the regular cross-section at the Wesenitz. In addition, using the average velocity coefficient is adverse because the irregular profile shape indicates a changing coefficient (Kim et al., 2008). ~~The higher error of the flow velocity estimation from the terrestrial camera images due to the unfavourable perspective in the far reach of the camera also leads to highest deviations of discharge compared to the UAV imagery~~.

Another important issue that needs to be noted is the circumstance that the image-based discharge estimation reveals a high variability that is sensitive to the defined wetted cross-section extracted with the defined water level. For instance, at the Wesenitz already 1 cm offset in the water level value causes a discharge difference of 0.08 m³/s (3 %) and 3 cm cause a

difference of 7 % (0.2 m³/s). Different studies already highlight that the correct water level is important for accurate discharge estimation due to the wetted cross-section area error but that it is less relevant for the accuracy of the flow velocities due to erroneous ortho-rectification (Dramais et al., 2011, Le Boursicaud et al., 2016, Leitao et al., 2018).

3.5. Limits and perspectives

In this study, a workflow for surface flow velocity and discharge measurements in rivers using terrestrial and UAV imagery was tested successfully. In general, three main processing steps are necessary, i.e. retrieving terrain information via SfM photogrammetry, estimating the flow velocity with PTV and eventually calculating the discharge with the information from both previous steps. However, some constraints need to be considered. The FlowVelo tool requires at least the video frames, the camera pose (either estimated within in the tool considering GCP information or provided externally), the water level and some estimates of the interior camera geometry (at least focal length and sensor size and resolution are needed). Furthermore, if the camera was not stable during the image acquisition, camera movements can be corrected automatically if sufficient shore areas are visible in the frames. With this information and pre-processing scaled river surface velocities are retrievable fully automatically.

However, some characteristics of the tool have to be considered. One aspect is the shore visibility in the frames for the co-registration. To guarantee large enough stable areas at larger rivers increasing the flying height might be necessary, potentially reducing the visibility of features to track. Alternatively, cameras with wider opening angles might be needed, potentially resulting in stronger lens distortions. Another important factor of the image velocimetry tool to consider is the impact of the choices of thresholds on processing time. On the one hand, the more often features are detected and the more frames they are tracked across, the more reliable and robust tracking results are possible because track filtering will receive a larger sample for processing. However, tracking more features across an increased number of frames also increases processing time significantly, which is especially relevant for cameras with high frame rates and image resolutions. Nevertheless, in this study the maximum processing time (for the terrestrial cameras at the Wesenitz that captured videos with lengths of about half a minute) was still below 5 minutes on an average computer.

Measuring surface velocities implies sensitivities to external impacts such as winds, waves, or raindrops, potentially falsifying an already established ratio between surface and average flow velocity, i.e. velocity coefficient, due to decreasing or increasing the surface velocity depending on the wind and wave direction and velocity. However, windy and rainy conditions should be avoided using any surface velocity measurement. The accuracy and reliability of the surface velocity measurement can be improved by adding traceable particles to increase the seeding density as shown by Detert et al. 2017. In this study, only natural particles floating at the river surfaces at both study areas were used, which did not cover the entire observed cross-section leading to data gaps complicating the retrieval of discharge from the sparsely distributed velocity values.

However, the FlowVelo tool does not provide discharge information, yet, because discharge estimation requires additional parameters, which need to be determined prior using image velocimetry as an accurate automatic remote sensing approach.

For instance, the water level and the related cross sectional area are needed as well as the velocity coefficient has to be known, which is a point of uncertainty especially at irregular river reaches. In this study, the velocity coefficient was estimated from the ADCP measurements dividing the mean velocity of the cross-section with the average surface velocity. However, alternative approaches, e.g. hydraulic modelling, should be analysed in more detail in future studies to evaluate if they can support the retrieval of more suitable velocity coefficients. This becomes especially interesting due to novel possibilities of high resolution bathymetric and topographic data, e.g. using SfM approaches for river mapping.

Conclusion

In this study, we introduce a remote sensing workflow for automatic flow velocity calculation and discharge estimation. The approach can be applied to terrestrial as well as aerial imagery. Thus, the importance of the acquisition scheme is secondary. However, visibility of tracked particles across the entire river cross-section is relevant as indicated by comparison of three different terrestrial cameras observing nearly the same river reach but revealing variations in the velocity estimates.

Camera movements during the video acquisition are stabilized using an automatic image co-registration method. To estimate flow velocity, particles on the water surface are detected and tracked using PTV. A feature search area is defined automatically solely relying on information about the water level and the topography of the river reach. The detected and tracked particles are filtered with cluster analysis and by making assumptions about the flow characteristics. Discharge is retrieved using the depth-averaged flow velocity and the wetted cross-section, which is derived from a 3D surface model reconstructed with multi-media photogrammetry applied to UAV imagery.

Two study sites have been observed with different terrestrial cameras and with a UAV platform. Comparing the results with ADCP reference measurements reveal a high accuracy potential for surface flow velocities calculated with PTV and automatic image co-registration, especially at standard gauging setups (maximal error of 4 %). At irregular cross-sections accuracy assessment of velocity tracking is limited due to high demands of position accuracies of the reference measurements. Discharge estimates with maximal errors of 5 % could be achieved at the standard track cross-section. At irregular profiles discharge calculation reveals significantly higher differences to reference measurements of 7 - 31 %. This is, amongst other reasons, due to incomplete velocity measurements across the entire river cross-section, leading to discharge overestimation when tracks are only retrieved in the faster flowing river region. Thus, further improvements of the tool for irregular cross-sections as well as considering artificial flow seeding is advisable in future studies.

The workflow, including the provided velocity tracking tool FlowVelo_Ttool, allows for a contact-less measurement of spatially distributed surface velocity fields and to estimate river discharge in previously ungauged and unmeasured regions, making it especially suitable for applications to assess flood events.

Code and data availability. The data used in this study and the tracking tool FlowVeloTool are available at http://dx.doi.org/10.25532/OPARA-32 and https://github.com/AnetteEltner/FlowVeloTool, respectively.

Author contributions. AE conceptualized the study, wrote the Python tool and drafted the manuscript. AE, HS, JG acquired, processed and analysed the data. HS and JG reviewed the draft.

Competing interests. The authors declare no competing interests.

Acknowledgements. We thank the European Social Fund (ESF) for funding this project (grants 100270097 and 100235479). These investigations are part of the research project "extreme events in small and medium catchments (EXTRUSO)." Furthermore, we are grateful for provided data sources by Andreas Kaiser and the Saxon state company for environment and agriculture. And we thank André Kutscher for helpful input the tracking toolbox. The data used in this study and the tracking tool FlowVelo tool are available at OPARA and https://github.com/AnetteEltner/FlowVeloTool, respectively.

References

Adler, M. (1993). Messungen von Durchflüssen und Strömungsprofilen mit einem Ultraschall-Doppler-Gerät (ADCP). Wasserwirtschaft, ,83(4), 192–196.

Blois, G., Best, J. L., Christensen, K. T., Cichella, V., Donahue, A., Hovakimyan, N., Pakrasi, I. (2016). UAV-based PIV for quantifying water-flow processes in large-scale natural environments. In 18th International Symposium on the Application of Laser and Imaging Techniques to Fluid Mechanics.

Bradski, G. (2000). The OpenCV Library. Dr. Dobb's Journal of Software Tools.

Brevis, W., Niño, Y., Jirka, G. H. (2011). Integrating cross - correlation and relaxation algorithms for particle tracking velocimetry. Experiments in Fluids, 50(1), 135 – 147.

Costa, J. E., Spicer, K. R., Cheng, R. T., Haeni, F. P., Melcher, N. B., Thurman, E. M., Plant, W.J., Keller, W. C. (2000). Measuring stream discharge by non-contact methods: A proof-of-concept experiment. Geophysical Research Letters, 4, 553–556.

Creutin, J. D., Muste, M., Bradley, A. A., Kim, S. C., & Kruger, A. (2003). River gauging using PIV techniques: a proof of concept experiment on the Iowa River. Journal of Hydrology, 277, 182–194.

Detert, M., Johnson, E. D., & Weitbrecht, V. (2017). Proof-of-concept for low-cost and non-contact synoptic airborne river flow measurements. International Journal of Remote Sensing, 38(8–10), 2780–2807.

Dietrich, J. T. (2017). Bathymetric Structure-from-Motion: extracting shallow stream bathymetry from multi-view stereo photogrammetry. Earth Surface Processes and Landforms, 42(2), 355–364.

Dramais, G., Le Coz, J., Camenen, B., & Hauet, A. (2011). Advantages of a mobile LSPIV method for measuring flood discharges and improving stage-discharge curves. Journal of Hydro-Environment Research, 5(4), 301–312.

Eltner, A., Kaiser, A., Castillo, C., Rock, G., Neugirg, F., & Abellan, A. (2016). Image-based surface reconstruction in geomorphometry – merits, limits and developments. Earth Surface Dynamics, 4, 359–389.

Eltner, Anette, Elias, M., Sardemann, H., & Spieler, D. (2018). Automatic Image-Based Water Stage Measurement for Long- Term Observations in Ungauged Catchments. Water Resources Research, (54), WR023913.

Eltner, Anette, & Schneider, D. (2015). Analysis of Different Methods for 3D Reconstruction of Natural Surfaces from Parallel-Axes UAV Images. The Photogrammetric Record, 30(151), 279–299.

Fischler, M. A., Bolles, R. C. (1981). Random sample consensus: a paradigm for model fitting with applications to image analysis and automated cartography. Communications of the ACM, 24(6), 381-395.

Fujita, I., Muste, M., Kruger, A. (1998). Large-scale particle image velocimetry for flow analysis in hydraulic engineering applications. Journal of Hydraulic Research, 36(3), 397-414.

Fujita, I., Watanabe, H., & Tsubaki, R. (2007). Development of a non - intrusive and efficient flow monitoring technique : The space - time image velocimetry (STIV). International Journal of River Basin Management ISSN:, 5, 105–114.

Fujita, I., Notoya, Y., Shimono, M. (2015). Development of UAV-based river surface velocity measurement by STIV based on high-accurate image stabilization techniques. E-proceedings of the 36th IAHR World Congress.

Genç, O., Ardıçlıoğlu, M., & Necati, A. (2015). Calculation of mean velocity and discharge using water surface velocity in small streams. Flow Measurement and Instrumentation, 41, 115–120.

Gravelle, R. (2015). Discharge Estimation: Techniques and Equipment. In: Geomorphological Techniques, Chap. 3, Sec. 3.5, British Society for Geomorphology.

Guillén, F., Patalano, A., García, C. M., & Bertoni, J. C. (2017). Use of LSPIV in assessing urban flash flood vulnerability. Natural Hazards, 87, 383–394.

Gunawan, B., Sun, X., Sterling, M., Shiono, K., Tsubaki, R., Rameshwaran, P., & Knight, D. W. (2012). The application of LS-PIV to a small irregular river for inbank and overbank flows. Flow Measurement and Instrumentation, 24, 1–12.

Harris, C., Stephens, M. (1988). A Combined Corner and Edge Detector. In: Proc. of 4th Alvey Vision Conference, 147-155.

Hauet, A., Kruger, A., Krajewski, W. F., Bradley, A., Muste, M., Creuting, J.-D., Wilson, M. (2008). Experimental System for Real-Time Discharge Estimation Using an Image-Based Method. Journal of Hydrologic Engineering, 13(2), 105–110.

Herschy, R. W. (2008). Streamflow Measurement. CRC Press, 3rd edition, 510 pp.

James, M., Chandler, J., Eltner, A., Fraser, C., Miller, P., Mills, J., Noble, T., Robson, S., Lane, S. (2019). Guidelines on the use of Structure from Motion Photogrammetry in Geomorphic Research.

Kim, Y., Muste, M., Hauet, A., Krajewski, W. F., Kruger, A., & Bradley, A. (2008). Stream discharge using mobile large-scale particle image velocimetry: A proof of concept. Water Resources Research, 44, W09502.

Koutalakis, P., Tzoraki, O., & Zaimes, G. (2019). UAVs for Hydrologic Scopes : Application of a Low-Cost UAV to Estimate Surface Water Velocity by Using Three Different Image-Based Methods. Drones, 3(14).

Le Boursicaud, R., Pénard, L., Hauet, A., Thollet, F., & Le Coz, J. (2016). Gauging extreme floods on YouTube: Application of LSPIV to home movies for the post-event determination of stream discharges. Hydrological Processes, 30, 90–105.

Le Coz, J., Hauet, A., Pierrefeu, G., Dramais, G., & Camenen, B. (2010). Performance of image-based velocimetry (LSPIV) applied to flash-flood discharge measurements in Mediterranean rivers. Journal of Hydrology, 394, 42–52.

Le Coz, Jérôme, Patalano, A., Collins, D., Guillén, N. F., García, C. M., Smart, G. M., Bind, J., Chiaverini, A., Le Boursicaud, R.L., Dramais, G., Braud, I., Braud, I. (2016). Crowdsourced data for flood hydrology: Feedback from recent citizen science projects in Argentina, France and New Zealand. Journal of Hydrology, 541, 766–777.

Legout, C., Darboux, F., Hauet, A., Esteves, M., Renaux, B., Denis, H., & Cordier, S. (2012). High spatial resolution mapping of surface velocities and depths for shallow overland flow. Earth Surface Processes and Landforms, 73, 984–993.

Leitão, J. P., Peña-haro, S., Lüthi, B., Scheidegger, A., Moy, M., & Vitry, D. (2018). Urban overland runo ff velocity measurement with consumer-grade surveillance cameras and surface structure image velocimetry. Journal of Hydrology, 565(June), 791–804.

Lewis, Q., Rhoads, B. (2015). Resolving two-dimensional flow structure in rivers using large-scale particle image velocimetry: An example from a stream confluence. Water Resources Research, 51, 7977–7994.

Lowe, D. (2004). Distinctive Image Features from Scale-Invariant Keypoints. International Journal of Computer Vision, 60(2), 91-110.

Lucas, B. D., Kanade, T. (1981). An iterative image registration technique with an application to stereo vision. IJCAI, 121-130.

Luhmann, T., Robson, S., Kyle, S., Boehm, J. (2014). Close-Range Photogrammetry and 3-D Imaging, 2nd edition, De Gruyter, Berlin, Germany, 683 pp.

Merz, J. (2010). Discharge Measurements in Low Flow Conditions With ADCP Technology – First Experiences in Nepal. Journal of Hydrology and Meteorology, 7 (1), 40-48.

Morgenschweis, G. (~~2011~~2010). Hydrometrie, Springer-Verlag Berlin Heidelberg, 582 pp.

Mulsow, C., Kenner, R., Bühler, Y., Stoffel, A., & Maas, H.-G. (2018). Subaquatic digital elevation models from UAV-imagery. International Archives of the Photogrammetry, Remote Sensing and Spatial Information Science, XLII-2, 739-744.

Muste, M., Fujita, I., & Hauet, A. (2008). Large-scale particle image velocimetry for measurements in riverine environments. Water Resources Research, 44, W00D14.

Muste, M., Hauet, A., Fujita, I., Legout, C., & Ho, H. C. (2014). Capabilities of large-scale particle image velocimetry to characterize shallow free-surface flows. Advances in Water Resources, 70, 160–171.

Muste, M., Ho, H., & Kim, D. (2011). Considerations on direct stream flow measurements using video imagery: Outlook and research needs. Journal of Hydro-Environment Research, 5, 289–300.

Patalano, A., Marcelo Garcia, C., Rodriguez, A. (2017). Rectification of Image Velocity Results (RIVeR): A simple and user-friendly toolbox for large scale water surface Particle Image Velocimetry (PIV) and Particle Tracking Velocimetry (PTV). Computers & Geosciences, 109, 323-33.

Perks, M. T., Russell, A. J., & Large, A. R. G. (2016). Technical note : Advances in flash flood monitoring using unmanned aerial vehicles (UAVs). Hydrology and Earth System Sciences, 20, 4005–4015.

Puleo, J. A., Mckenna, T. E., Holland, K. T., & Calantoni, J. (2012). Quantifying riverine surface currents from time sequences of thermal infrared imagery. Water Resources, 48, W01527.

Ran, Q. H., Li, W., Liao, Q., Tang, H. L., & Wang, M. Y. (2016). Application of an automated LSPIV system in a mountainous stream for continuous flood flow measurements. Hydrological Processes, 30, 3014–3029.

Rublee, E., Rabaud, V., Konolige, K., & Bradski, G. (2011). ORB: An efficient alternative to SIFT or SURF. IEEE International Conference on Computer Vision (ICCV).

Sidorchuk, A., Schmidt, J., & Cooper, G. (2008). Variability of shallow overland flow velocity and soil aggregate transport observed with digital videography. HYDROLOGICAL PROCESSES, 22, 4035–4048.

Stumpf, A., Augereau, E., Delacourt, C., & Bonnier, J. (2016). Photogrammetric discharge monitoring of small tropical mountain rivers: A case study at Rivière des Pluies, Réunion Island. Water Resources Research, 52, WR018292.

Tauro, F., Piscopia, R., & Grimaldi, S. (2017). Streamflow Observations From Cameras: Large-Scale Particle Image Velocimetry or Particle Tracking Velocimetry? Water Resources Research, 53, 10374–10394.

Tauro, Flavia, Petroselli, A., & Arcangeletti, E. (2016). Assessment of drone-based surface fl ow observations. HYDROLOGICAL PROCESSES, 30, 1114–1130.

Tauro, Flavia, Tosi, F., Mattoccia, S., Toth, E., Piscopia, R., & Grimaldi, S. (2018). Optical Tracking Velocimetry (OTV): Leveraging Optical Flow and Trajectory-Based Filtering for Surface Streamflow Observations. Remote Sensing, 10, rs10122010.

Thielicke, W., Stamhuis, E. (2014). PIVlab - Towards User-friendly, Affordable and Accurate Digital Particle Image Velocimetry in MATLAB. Journal of Open Research Software, 2, e30.

Thumser, P., Haas, C., Tuhtan, J. A., Fuentes-Pérez, J. F., & Toming, G. (2017). RAPTOR-UAV: Real-time particle tracking in rivers using an unmanned aerial vehicle. Earth Surface Processes and Landforms, 42, 2439–2446.

Tsubaki, R., Fujita, I., Tsutsumi (2011). Measurement of the flood discharge of a small-sized river using an existing digital video recording system. Journal of Hydro-environment Research, 5, 313-321.

Welber, M., Le Coz, J., Laronne, J., Zolezzi, G., Zamler, D., Dramais, G., Hauet, A., Salvaro, M. (2016). Field assessment of noncontact stream gauging using portable surface velocity radars (SVR). Water Resources Research, 52, WRO17906.

Woodget, A. S., Carbonneau, P. E., Visser, F., & Maddock, I. P. (2015). Quantifying submerged fluvial topography using hyperspatial resolution UAS imagery and structure from motion photogrammetry. Earth Surface Processes and Landforms, 40(1), 47–64.

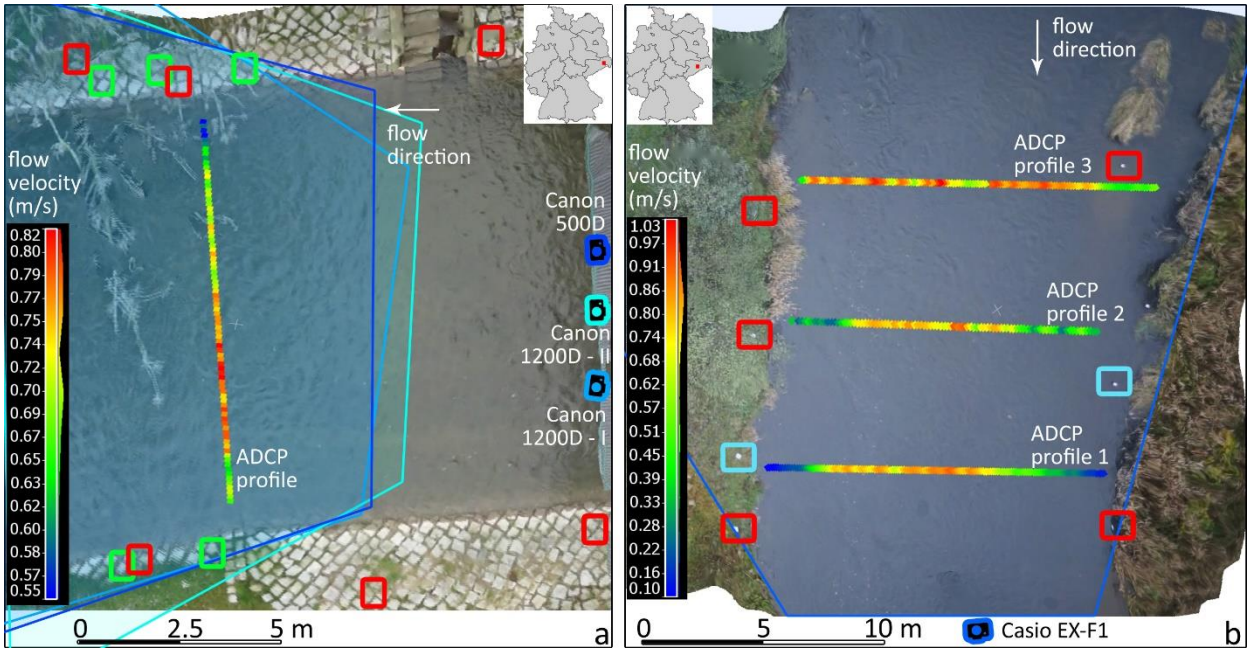

Figure 1: Areas of interest at the Wesenitz (a) and the Freiberger Mulde (b) displayed with UAV orthophotos calculated from video frames. Surface flow velocities measured with an ADCP and the corresponding locations of the measurement cross-sections within the river are illustrated. Ground control points (GCPs) are used to reference the image data at both river reaches. Red squares highlight GCPs used for terrestrial and UAV data at the Freiberger Mulde and UAV data at the Wesenitz. Green squares show location of GCPs used for terrestrial imagery at the Wesenitz. Check points (blue squares) are used to assess the accuracy of the 3D reconstruction from video frames at the Freiberger Mulde. Camera locations of the terrestrial image sequence acquisition are illustrated as pictograms and corresponding image extent areas are shown (displayed area of interests in RGB correspond to the aerial image extents). ~~.~~

Table 1: River velocities measured with ADCP

	Profile	Mean velocity (m/s)	Mean surface velocity (m/s)	Max. surface velocity (m/s)	Velocity coefficient (-)	Cross-section area (m²)	Discharge (m²/s)
Wesenitz	-	0.59	0.70	0.82	0.84	4.63	2.72
Freiberger Mulde	1	0.48	0.60	0.92	0.80	11.75	5.60
	2	0.58	0.70	0.93	0.83	10.45	6.01
	3	0.59	0.76	1.03	0.78	10.30	6.04

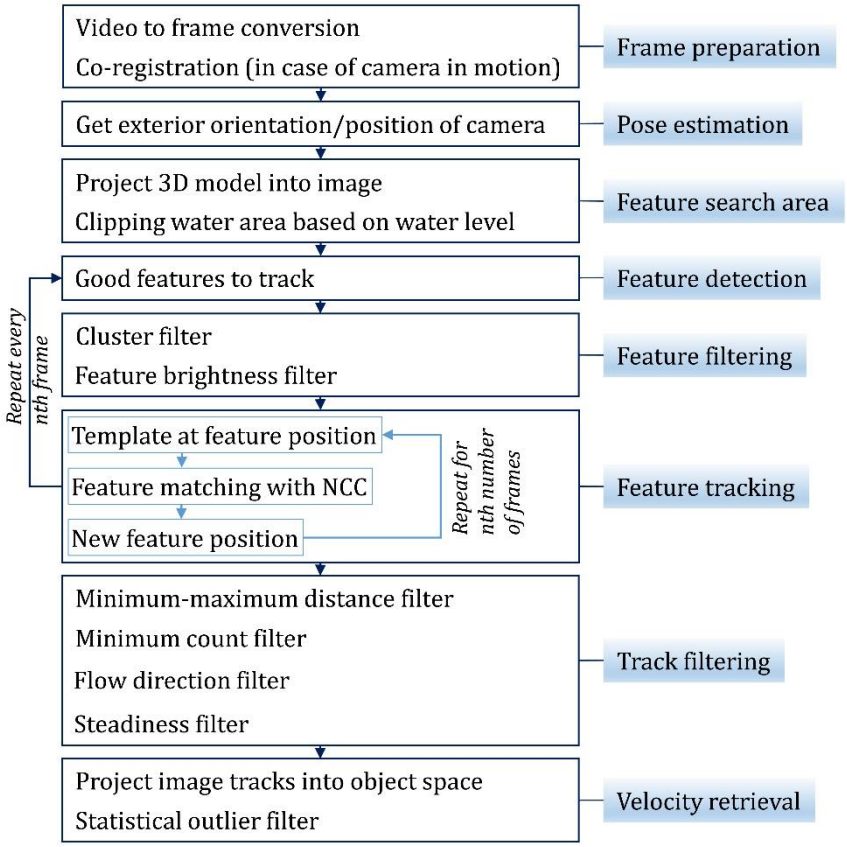

Figure 2: Workflow to retrieve flow velocities from video sequences.

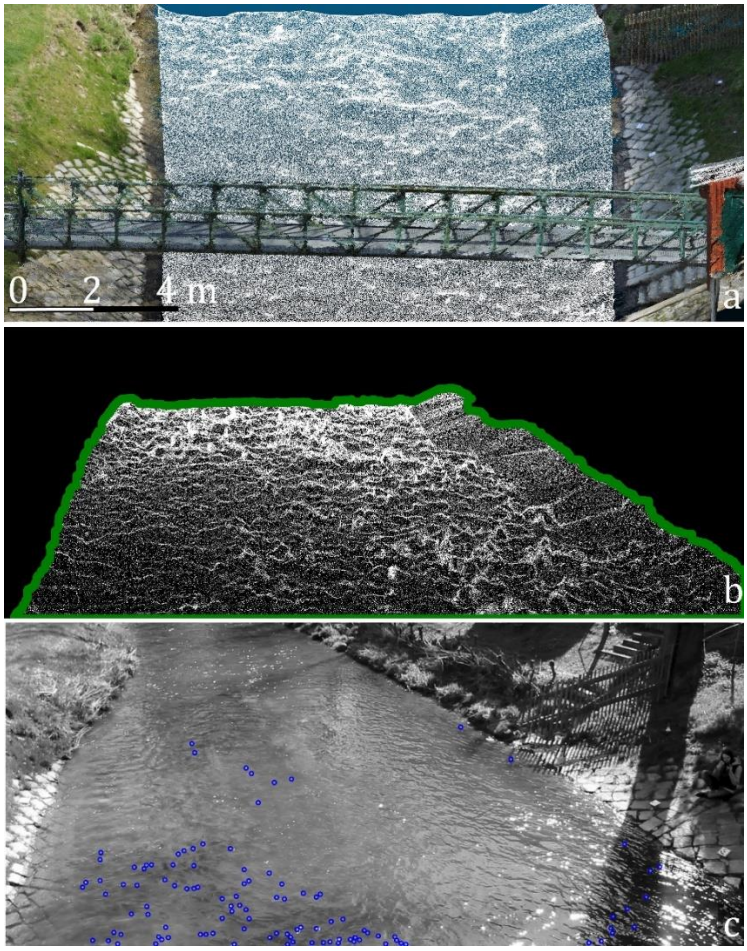

Figure 3: Defining the search area to extract particles to track. a) 3D point cloud of the investigated river reach at the Wesenitz. Coloured points (colorized according to their object colour) are 3D points above the water surface reconstructed with SfM photogrammetry. White points are 3D points below the water surface reconstructed with SfM and corrected for refraction effects. b) 3D point cloud below the water level projected into image space. Green line depicts contour line, which is used as search mask for feature detection. c) Detected and filtered features considered for tracking (blue circles).

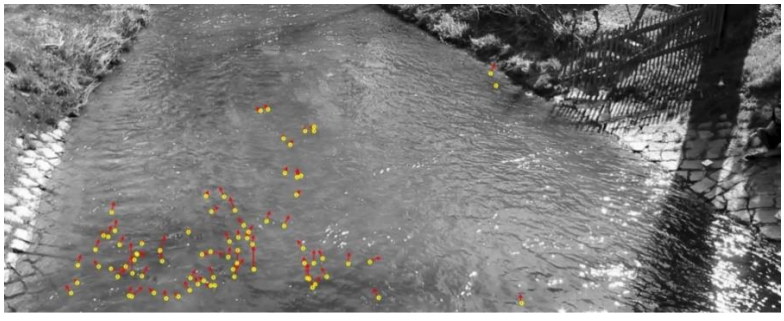

Figure 4: Exemplary display of the tracking result from one frame to the next.

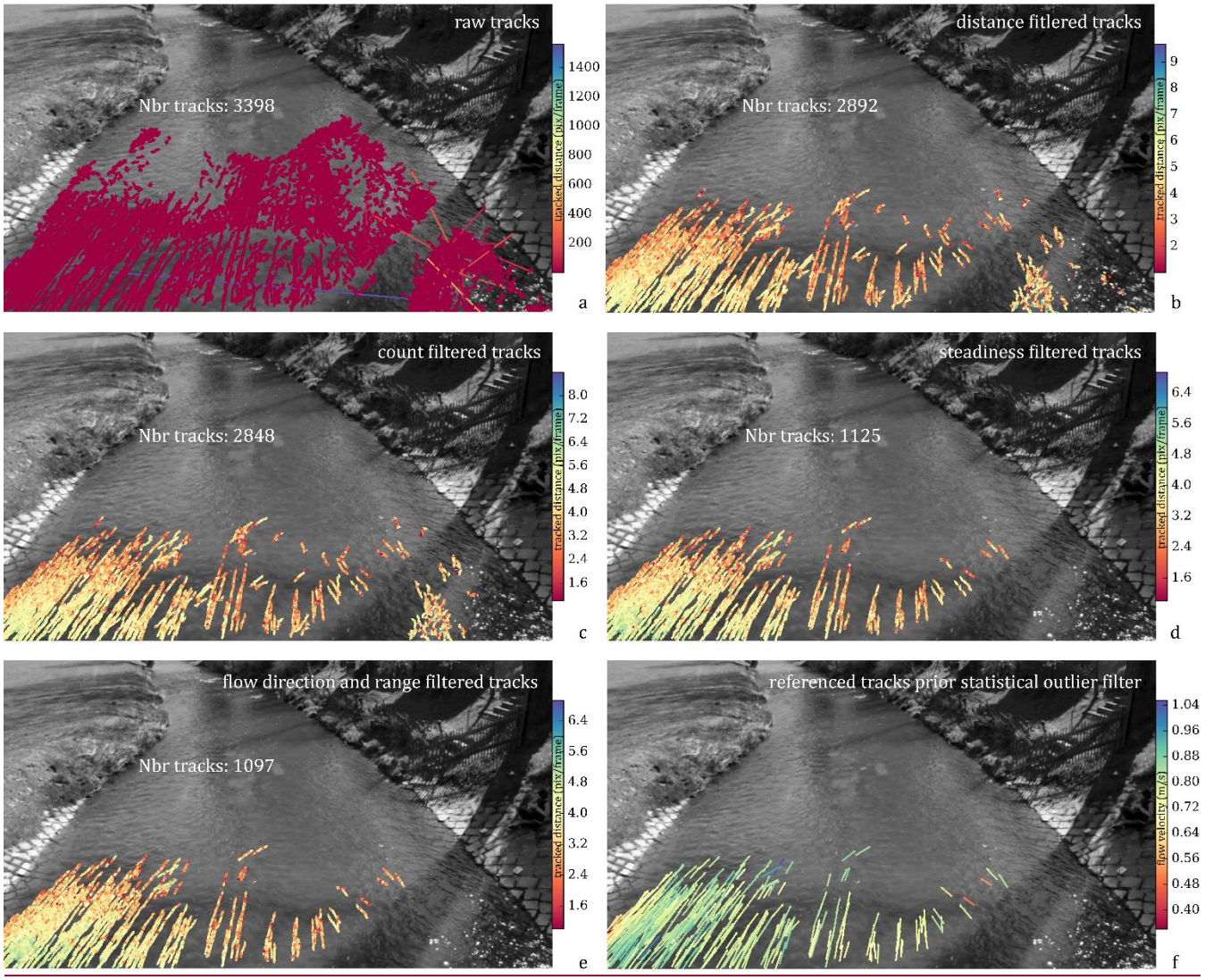

Figure 5: Result of tracked features after filtering has been applied to the video sequence of camera ~~1200D~~500D ~~I~~ (with a temporal length of ~~28~~ 23 seconds). Sub-tracks are displayed and the number of tracks refers to full tracks (combination of sub-tracks). a) Raw tracks prior any filtering. b) Filtered tracks after applying minimum and maximum distance thresholds. c) Filtered tracks after applying a minimum count of sub-tracks over which features need to be tracked. d) Filtered tracks after considering standard deviation of sub-track directions. e) ~~f~~Filtered tracks after considering ~~low direction characteristics (i.e.~~ deviation from average flow direction~~, standard deviation of sub-track directions,~~ and range of sub-track directions~~)~~. f) Filtered tracks converted into metric values to receive flow velocities in the unit m/s.

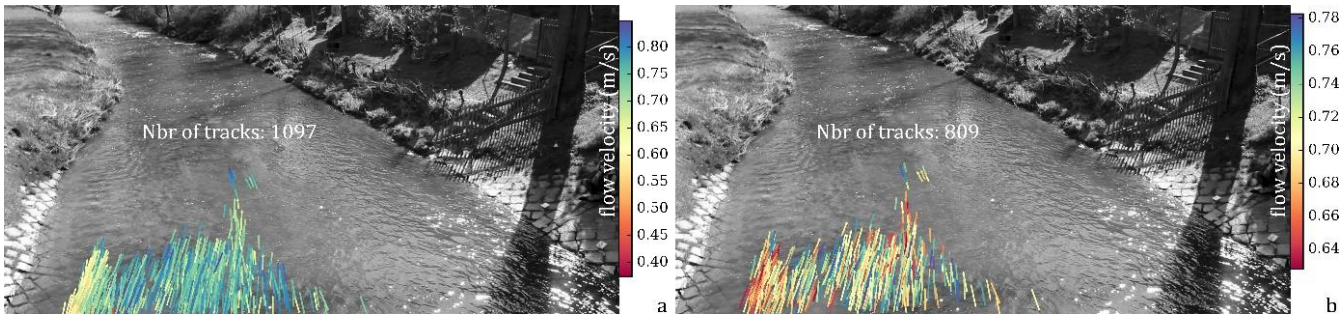

Figure 56: Filtered tracks converted into metric values to receive flow velocities in the unit m/s. a) Referenced flow velocity tracks. b) Statistically filtered final flow velocities.

Table 12: Accuracy of camera pose estimation and density of tracking results. s0 corresponds to the average reprojection error after the adjusted spatial resection.

		accuracy				tracking density		
		standard deviation (m)			s0 (pixel)	number of frames	number of raw tracks	number of final tracks
		X	Y	Z				
Wesenitz	UAV camera	0.172	0.274	0.162	2.71.1	78	271	58
	500D	0.027	0.066	0.039	3.10.9	690	3552	439
	1200D-I	0.042	0.169	0.080	7.93.2	700	4781	603
	1200D-II	0.041	0.127	0.073	4.01.6	640	14786	1239
Frei. Muld.	UAV camera	0.085	0.078	0.031	1.30.5	73	844	126
	Casio EX-F1	0.018	0.010	0.015	1.10.3	750	3886	334

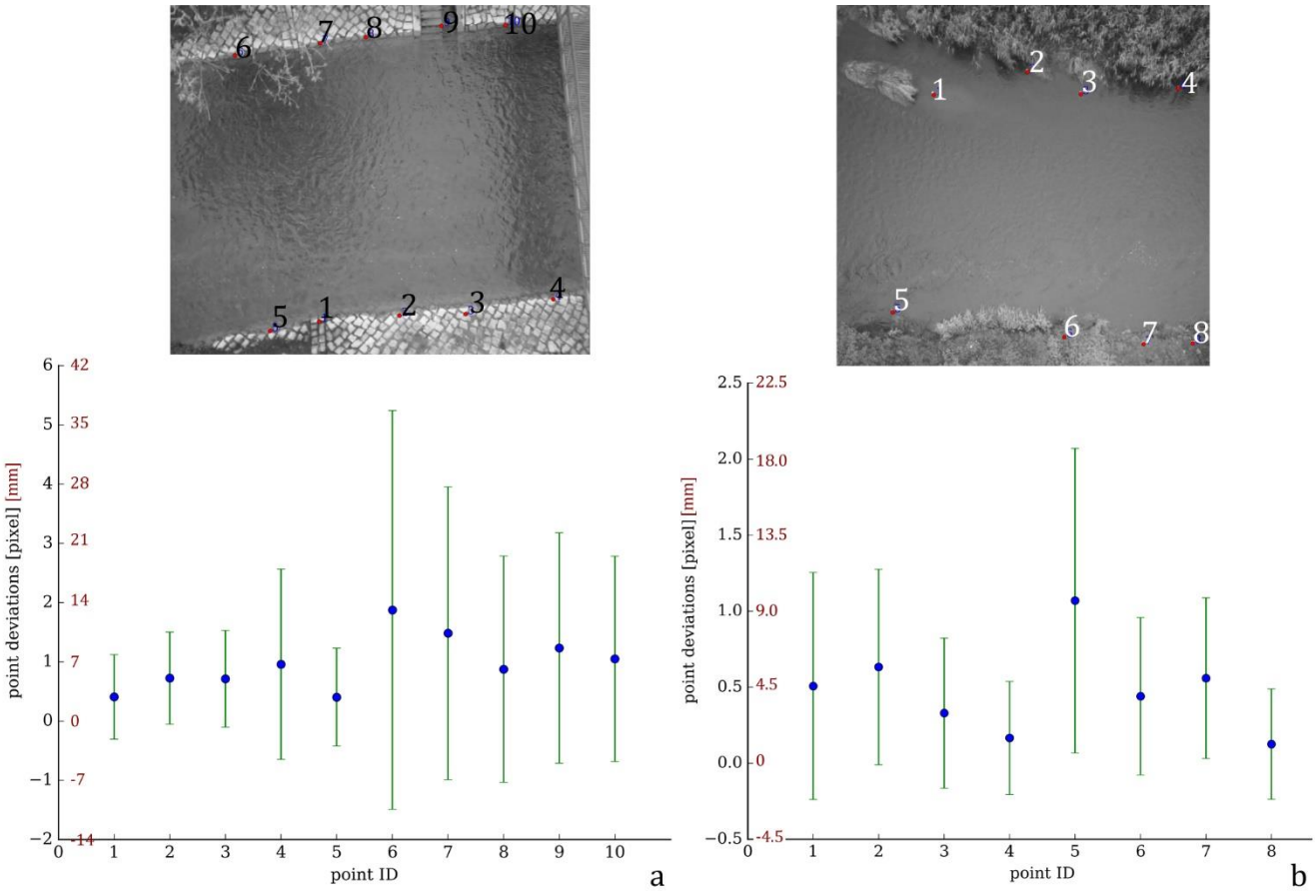

Figure 5~~7~~6: Accuracy of co-registration of video frames to single master frame displayed in image space (black axis) and the corresponding accuracy in object space (red axis) at the river Wesenitz (a) and Freiberger Mulde (b). Note that the images are only extracts form the original (bigger) images.

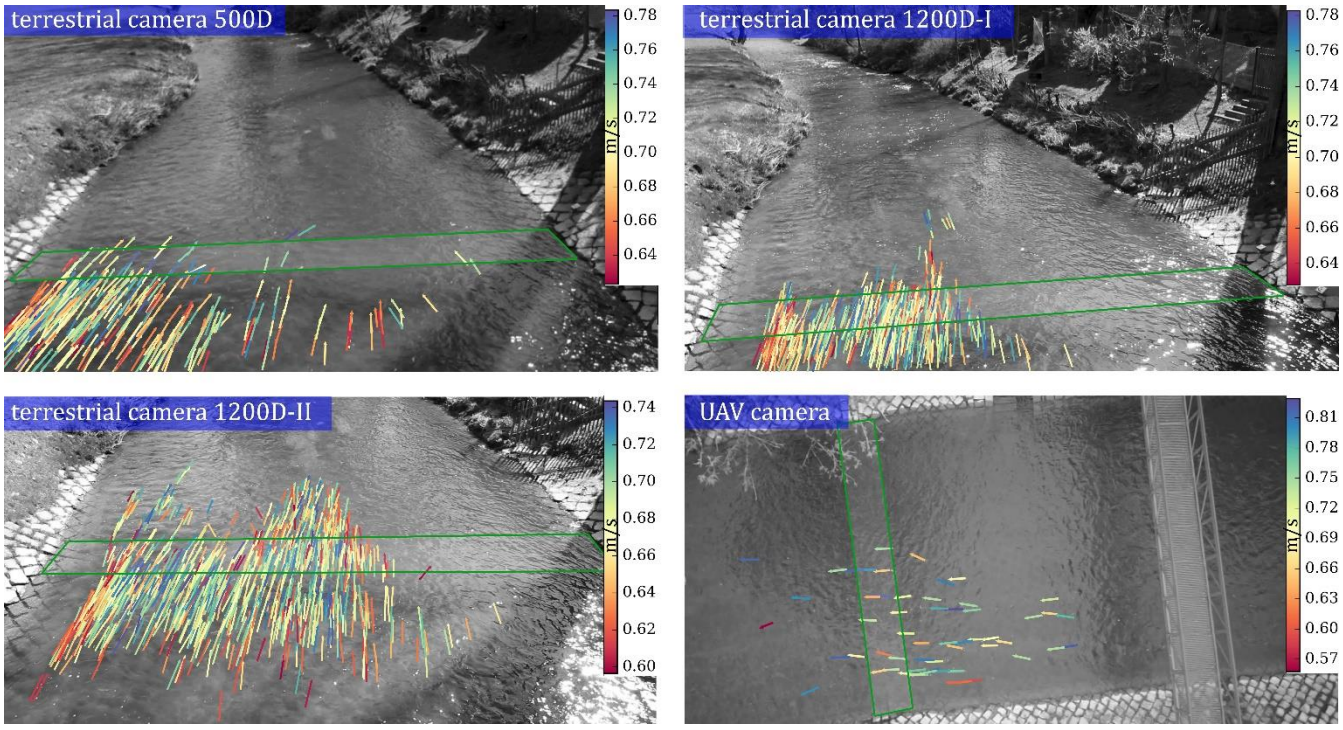

Figure 5~~8~~7: Flow velocities estimated at the Wesenitz using video frames captured with three different terrestrial cameras and a camera on an UAV platform. Final tracks after statistical outlier filter (fig. 5f) are displayed. Green border indicates area, in which image-based measurements are compared to ADCP velocities.

Table 2~~3~~: Deviation between ADCP measurements and video based flow velocities. Differences are calculated for tracks within a range of 1 m and closest to the ADCP measurements.

			surface velocity difference [m/s]		
			average	standard deviation	track count
Wesenitz	UAV camera		0.03	0.07	10
	500D		0.00	0.06	24
	1200D-I		0.02	0.07	56
	1200D-II		0.08	0.06	88
	average		0.03	0.06	-
Freiberger Mulde	UAV camera	profile 1	0.03	0.09	8
	UAV camera	profile 2	0.01	0.06	8
	UAV camera	profile 3	-0.05	0.06	8
	Casio EX-F1	profile 1	-0.01	0.05	10
	average		0.01	0.07	-

Table 34: Discharge estimated using flow velocities and cross-sections retrieved from UAV data.

			average surface flow velocity at the cross-section [m/s]	Cross-section area [m²]	Discharge[m³/s]	
					Average	Standard deviation
Wesenitz	UAV camera		0.71	4.57	2.73	0.27
	500D		0.72		2.76	0.15
	1200D-I		0.71		2.72	0.16
	1200D-II		0.67		2.58	0.16
	average				2.70	0.18
	std dev				0.08	
Freiberger Mulde	UAV camera	profile 1	0.79	11.61	7.34	0.74
		profile 2	0.77	10.35	6.60	0.60
		profile 3	0.79	9.19	5.64	0.43
	Casio EX-F1	profile 1	0.76	11.61	7.06	0.46
	average				6.66	0.56
	std dev				0.75	

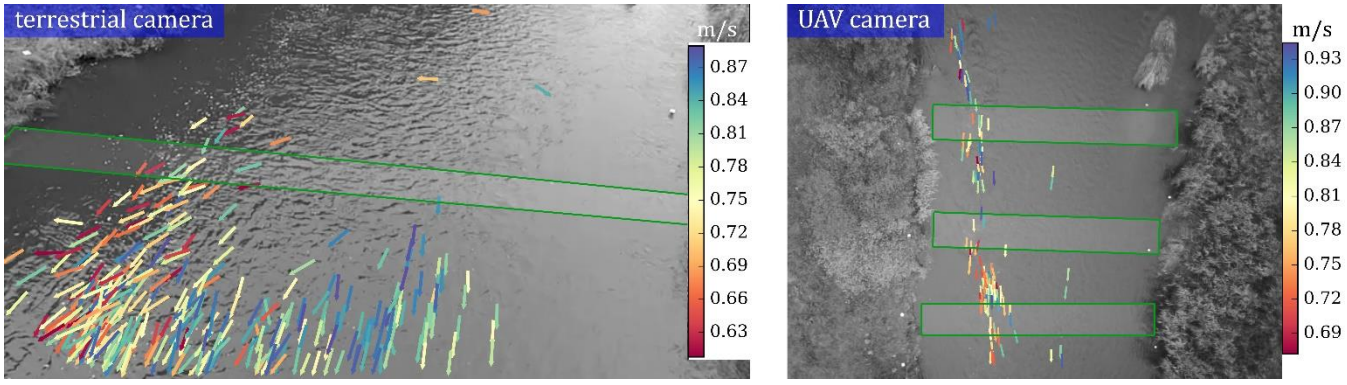

Figure 598: Flow velocities estimated at the Freiberger Mulder using video frames captured with a terrestrial camera and a camera on an UAV platform. Green border indicates area, in which image-based measurements are compared to ADCP velocities.

Appendix A1: Accuracy of the estimation of the exterior camera geometry via spatial resection

			nbr observations (GCPs used)	s0 [mm]	X [mm]	Y [mm]	Z [mm]	omega [rad]	phi [rad]	kappa [rad]	pixel size [mm]
Freiberger Mulde	UAV camera	estimated value	7	0.006	14993	18976	30033	-0.011	0.013	2.483	0.012
		std dev estimated value			85	78	31	0.002	0.002	0.001	
	Casio EX-F1	estimated value	6	0.003	6990	94615	6632	1.066	-0.446	2.995	0.011
		std dev estimated value			18	10	15	0.001	0.001	0.001	
Wesenitz	UAV camera	estimated value	6	0.036	203874	196051	215766	-0.264	-0.022	0.149	0.012
		std dev estimated value			172	274	162	0.015	0.009	0.003	
	500D	estimated value	5	0.015	199731	188229	202939	0.537	-1.126	2.115	0.017
		std dev estimated value			27	66	39	0.012	0.003	0.011	
	1200D-I	estimated value	5	0.037	199546	191415	202847	0.020	-1.270	1.638	0.012
		std dev estimated value			42	169	80	0.042	0.008	0.038	
	1200D-II	estimated value	4	0.019	199464	189855	203006	0.276	-0.989	1.918	0.012
		std dev estimated value	-	-	41	127	73	0.015	0.008	0.014	-

Appendix A2: Parameter settings chosen for each image-based tracking example in this study.

	UAV camera (Freiberger Mulde)	UAV camera (Wesenitz)	terrestrial camera (Casio-EX F1; Freiberger Mulde)	terrestrial cameras (500D, 1200D-I, 1200D-II; Wesenitz)
parameters feature detection				
threshold minimum brightness [8 bit]	120	130	170	135
search radius neighbouring features [pixel]	10	5	5	50
maximum neighbours in radius [ ]	10	5	5	10
maximum total number detected features [ ]	3000	3000	3000	3000
sensitivity (minimum quality detected feature) [ ]	0.005	0.002	0.002	0.002
parameters feature matching				
template width	10	6	10	10
template height	10	6	10	10
search area width	15	9	15	15
search area height	15	9	15	15
shift search area in x direction	0	-1	0	1
shift search area in y direction	1	0	1	0
subpixel measurement	TRUE	TRUE	TRUE	TRUE
perform LSM	FALSE	FALSE	FALSE	FALSE
parameters iterations				
detect features every nth frame	15	15	15	15
track features for nth number of frames	20	20	20	20
select every nth frame for tracking	1	1	1	1
parameter scaling				
frame rate (per second)	25	25	30	30
parameters track filtering				
minimum tracking distance [pixel]	0.1	0.1	0.1	0.1
maximum tracking distance [pixel]	10	10	10	10
minimum number of tracks (count) [ ]	13	13	13	13
steadiness [deg]	30	30	30	30
maximum range of directional change [deg]	120	120	120	120
maximum deviation from main flow direction [deg]	30	20	30	20
statistical outlier threshold [ ]	1.5	1.5	1.5	1.5